Title

Bolstering the Number and Function of HSV-1–Specific CD8+ Effector Memory T Cells and Tissue-Resident Memory T Cells in Latently Infected Trigeminal Ganglia Reduces Recurrent Ocular Herpes Infection and Disease

Journal

The Journal of Immunology, 199(1)

ISSN

0022-1767

Authors

Khan, Arif A
Srivastava, Ruchi
Chentoufi, Aziz A
et al.

Publication Date

2017-07-01

DOI

10.4049/jimmunol.1700145

Peer reviewed

HHS Public Access

Author manuscript

J Immunol. Author manuscript; available in PMC 2018 July 01.

Published in final edited form as:

J Immunol. 2017 July 01; 199(1): 186–203. doi:10.4049/jimmunol.1700145.

Bolstering the Number and Function of HSV-1-Specific CD8+ T_{EM} and T_{RM} cells in Latently Infected Trigeminal Ganglia Reduces Recurrent Ocular Herpes Infection and Disease

Arif A. Khan[1], **Ruchi Srivastava**[1], **Aziz A. Chentoufi**[1], **Elizabeth Kritzer**[1], **Sravya Chilukuri**[1], **Sumit Garg**[1], **David C. Yu**[1], **Hawa Vahed**[1], **Lei Huang**[1], **Sabrina A. Syed**[1], **Julie N. Furness**[1], **Tien T Tran**[1], **Nesburn B. Anthony**[1], **Christine E. McLaren**[2], **John Sidney**[3], **Alessandro Sette**[3], **Randolph J. Noelle**[4], and **Lbachir BenMohamed**[1,5,6,‡]

[1]Laboratory of Cellular and Molecular Immunology, Gavin Herbert Eye Institute, University of California Irvine, School of Medicine, Irvine, CA 92697

[2]Department of Epidemiology, University of California, Irvine, CA 92697

[3]Department of Vaccine Discovery, La Jolla Institute for Allergy and Immunology, La Jolla, CA 92037

[4]Department of Microbiology and Immunology, Geisel School of Medicine at Dartmouth, Lebanon, NH03755

[5]Department of Molecular Biology & Biochemistry; University of California Irvine, School of Medicine, Irvine, CA 92697, USA

[6]Institute for Immunology; University of California Irvine, School of Medicine, Irvine, CA 92697, USA

Abstract

Herpes simplex virus type 1 (HSV-1) is a prevalent human pathogen that infects over 3.72 billion individuals worldwide and can cause potentially blinding recurrent corneal herpetic disease. HSV-1 establishes latency within sensory neurons of trigeminal ganglia (TG) and TG-resident $CD8^+$ T cells play a critical role in preventing its reactivation. The repertoire, phenotype and function of protective $CD8^+$ T cells are unknown. Bolstering the apparent feeble numbers of $CD8^+$ T cells in TG remains a challenge for immunotherapeutic strategies. In this study, a comprehensive panel of 467 HLA-A*0201-restricted $CD8^+$ T cell epitopes were predicted from the entire HSV-1 genome. $CD8^+$ T cell responses to these genome-wide epitopes were compared in HSV-1 seropositive symptomatic (SYMP) individuals (with a history of numerous episodes of recurrent herpetic disease) vs. asymptomatic (ASYMP) individuals (who are infected but never experienced any recurrent herpetic disease). Frequent polyfunctional HSV-specific effector memory IFN-$\gamma^+CD107^{a/b+}CD44^{high}CD62L^{low}CD8^+$ T_{EM} cells were detected in ASYMP individuals and were mainly directed against three “ASYMP” epitopes. In contrast, SYMP individuals have more

‡Corresponding author: Professor Lbachir BenMohamed, Laboratory of Cellular and Molecular Immunology, Gavin Herbert Eye Institute; Hewitt Hall, Room 2032; 843 Health Sciences Rd; Irvine, CA 92697; Phone: 949-824-8937. Fax: 949-824-9626. Lbenmoha@uci.edu.

Conflict of interest: The authors have declared that no conflict of interest exists

mono-functional central memory $CD44^{high}CD62L^{high}CD8^{+}$ T_{CM} cells. Furthermore, therapeutic immunization with an innovative prime/pull vaccine, based on priming with multiple "ASYMP" epitopes (prime) and neurotropic TG delivery of the T-cell attracting chemokine CXCL-10 (pull), boosted the number and function of $CD44^{high}CD62L^{low}CD8^{+}$ T_{EM} and tissue-resident $CD103^{high}CD8^{+}$ T_{RM} cells in TG of latently infected HLA-A*0201 Tg mice and reduced recurrent ocular herpes following UV-B induced reactivation. These findings have profound implications in the development of T-cell-based immunotherapeutic strategies to treat blinding recurrent herpes infection and disease.

INTRODUCTION

A staggering 3.72 billion individuals worldwide (i.e. over 50% of the world population) are currently infected with herpes simplex type 1 (HSV-1), a neurotropic member of the alpha herpesvirus family that develops a "steady state" latent infection in the sensory neurons of trigeminal ganglia (TG) (1–3). The majority of infected individuals remain ASYMP (4–10). They do not experience any recurrent herpetic disease as they may have developed a "natural" protective immunity that helps reduce/suppress virus reactivation, symptomatic shedding, and/or recurrent herpes disease (10–12). In contrast, a much smaller population of SYMP individuals may have lost such "natural" immunity causing them to consequently develop frequent, recurrent herpetic disease (i.e. 2–5 episodes of recurrent disease/year) triggered by psychological, chemical, or physical stress (13–15). Although standard antiviral drug treatments (e.g. acyclovir) can reduce recurrent symptomatic disease to some extent, they do not clear the infection (16–20). An alternative immunotherapeutic herpes simplex vaccine is currently unavailable (reviewed in (12)). The efforts to develop a sub-unit immunotherapeutic vaccine throughout the past twenty years have only focused on 2 out of the 84^{+} proteins encoded by the HSV genome: glycoproteins gB and/or gD (21, 22). Clinical vaccine trials based on gB and/or gD have provided only moderate and transient protection in spite of inducing neutralizing antibodies and HSV-specific $CD4^{+}$ T cells (7, 12, 21, 22). This suggests that an effective immunotherapeutic herpes vaccine: (*i*) must include HSV antigens, other than gB and gD; and (*ii*) would likely require induction of strong antiviral $CD8^{+}$ T cell responses, in addition to neutralizing antibodies and $CD4^{+}$ T cell responses.

Direct evidence in animal models (6, 23, 24) and indirect observations in humans (25–27) indicates that after the clearance of primary HSV-1 infection, a pool of memory $CD8^{+}$ T cells develops and recirculates between secondary lymphoid organs and peripheral tissues while a different pool of memory $CD8^{+}$ T cells develops and resides within peripheral tissues (1, 5, 6, 10, 15, 17, 28–33). TG-resident $CD8^{+}$ T cells play a critical role in preventing HSV-1 reactivation from latently infected sensory neurons of TG and subsequent recurrent corneal herpetic disease (1, 10). Information on the repertoire, phenotype and function of protective $CD8^{+}$ T cells that reside in latently infected TG is essential to design immunotherapeutic strategies. We hypothesize that a sufficient number of functional $CD8^{+}$ T cells in TG of ASYMP individuals has likely resulted in the suppression (or abortion) of attempts of virus reactivation from latency and hence in elimination of symptomatic shedding and reduction of recurrent disease (34). In contrast, the lesser numbers of functional $CD8^{+}$ T cells in TG of SYMP individuals may not be sufficient to eliminate virus

reactivation, and would thereby result in repetitive symptomatic shedding and recurrent herpetic disease. Therefore, an immunotherapeutic vaccine strategy that increases the number of functional HSV-specific $CD8^+$ T cells in TG would logically prevent or reduce virus shedding in tears and should also reduce recurrent ocular herpetic disease. Despite extensive research efforts over two decades, this goal remains unattained so far, mainly because during latency, the TG appear to be an immunologically restrictive compartment that is not "open" to homing and sequestering of $CD8^+$ T cells that would migrate from the circulation (35). While $CD8^+$ T cells appeared to infiltrate the TG during acute infection (likely in response to high-levels of T cell-attracting chemokines, CXCL9, CXCL10 and CCL5), a drop in the levels of these chemokines during latency may prevent migration of sufficient numbers of antiviral $CD8^+$ T cells from the blood into latently infected TG. We further hypothesize that locally delivering the T cell-attracting chemokines, CXCL9, CXCL10 and CCL5, in latently infected TG would increase the size of local anti-viral $CD8^+$ T cell infiltrates which, in turn, would help reduce/suppress virus reactivation, symptomatic shedding, and/or recurrences of herpes disease.

In the present study, we employed a genome-wide analysis strategy and predicted a panel of 467 HSV-1 potential HLA-A*0201-restricted epitopes. Frequent polyfunctional effector memory HSV-specific IFN-γ^+CD107$^{a/b+}$CD44^{high}CD62L^{low}CD8$^+$ T_{EM} cells were detected in PBMC of ASYMP individuals and were directed mainly against three epitopes, $UL9_{196–204}$, $UL25_{572–580}$ and $UL44_{400–408}$. In contrast, HSV-specific $CD8^+$ T cells in PBMC of SYMP individuals were mainly of the central memory phenotype (CD44^{high}CD62L^{high}CD8$^+$ T_{CM} cells) and were directed against other non-overlapping epitopes. Furthermore, we demonstrate that bolstering the number of functional HSV-specific $CD8^+$ T_{EM} and tissue-resident CD103^{high}CD8$^+$ T_{RM} cells in latently infected TG of "humanized" HLA Tg mice through HSV-1 human epitopes/CXCL10-based prime/pull therapeutic vaccine protected against virus shedding and recurrent herpetic disease. These findings strongly suggest the feasibility of developing an effective prime/pull therapeutic herpes vaccine based on enhancing the number and function of existing HSV-specific memory $CD8^+$ T_{EM} and T_{RM} cells within latently infected sensory ganglia.

MATERIALS & METHODS

Human study population

During the last thirteen years (i.e. January 2003 to October 2016), we have screened 803 individuals for HSV-1 and HSV-2 seropositivity (Table IA). Five hundred fifty four individuals were White, 249 were non-White (African, Asian, Hispanic and other), 410 were female, and 393 were male. Among this sample, a cohort of 293 immuno-competent individuals, ranging from 21–67 years old (median 29), and were seropositive for HSV-1 and seronegative for HSV-2, were enrolled in the present study. All patients were negative for HIV and HBV, with no history of immunodeficiency. 722 patients were HSV-1, HSV-2 or HSV-1/HSV-2 seropositive, among which 658 patients were healthy and defined as asymptomatic (ASYMP). These individuals had never had any herpes disease, ocular, genital or dermal, based on self-reporting and clinical examination, individuals in the absence of therapy. Even a single episode of any herpetic disease would exclude the

individual from this group). The remaining 81 patients were defined as HSV-seropositive symptomatic (SYMP) individuals who suffered with frequent and severe recurrent genital, ocular and/or oro-facial lesions. Two of these SYMP patients had clinically well-documented repetitive herpes stromal keratitis (HSK) and another had 20 episodes over 20 years that required several corneal transplantations. Signs of recurrent disease in SYMP patients were defined as herpetic lid lesions, herpetic conjunctivitis, dendritic or geographic keratitis, stromal keratitis, and iritis consistent with HSK, with one or more episodes per year for the past 2 years. However, at the time of blood collection, SYMP patients had no recurrent disease (other than corneal scarring) and had had no recurrences during the past 30 days. They had no ocular disease other than HSK, had no history of recurrent genital herpes, and are HSV-1 seropositive and HSV-2 seronegative. Because the spectrum of recurrent ocular herpetic disease is wide, our emphasis is mainly on the number of recurrent episodes and not on the severity of the recurrent disease. No attempt was made to assign specific T cell epitopes to specific severity of recurrent lesions. Patients were also excluded if they: (1) had an active ocular (or elsewhere) herpetic lesion, or had one in the past 30 days, (2) are seropositive for HSV-2, (3) pregnant or breastfeeding, or (4) were on acyclovir or other related anti-viral drugs or any immunosuppressive drugs at time of blood draw. SYMP and ASYMP groups were matched for age, gender, serological status, and race. We also collected and tested blood samples from 81 healthy control individuals who were seronegative for both HSV-1 and HSV-2 and had no history of ocular herpes, genital lesions or oro-facial herpes disease. The actual number and characteristics of SYMP, ASYMP and seronegative individuals enrolled in the present study is shown in Table IB. All clinical investigations in this study have been conducted according to Declaration of Helsinki principles. All subjects were enrolled at the University of California Irvine under approved Institutional Review Board-approved protocols (IRB#2003-3111 and IRB#2009-6963). Written informed consent was received from all participants prior to inclusion in the study.

In silico prediction of potential human leukocyte antigen HLA-A*0201-restricted CD8$^+$ T cell epitopes from HSV-1 genome

The HSV-1 open reading frames (ORFs) utilized in this study were from strain 17 (NCBI accession number NC001806). We first searched the deduced amino acid sequence encoded by the entire HSV1 genome (strain 17) for potential HLA-A*0201-binding regions. Candidate HLA-A*0201-restricted epitopes were identified from all HSV-1 84$^+$ ORFs using previously described BIMAS software (Bioinformatics and Molecular Analysis Section, NIH (Washington, DC); (http://bimas.dcrt.nih.gov/molbio/hla_bind/) and the SYFPEITHI algorithm (http://www.syfpeithi.de/) (6). Potential cleavage sites for human proteasome were identified using NetChop 3.0 (http://www.cbs.dtu.dk/services/NetChop/) and MHC Pathway (http://www.mhc-pathway.net) for screening (6). These algorithms identified a total of 467 potential regions (i.e. CD8$^+$ T cell epitopes) with high predicted affinity to the HLA-A*0201 molecule (Suppl. Table S1). All epitopes are restricted to HLA-A*0201, a haplotype chosen for this study as it is represented in over 50% of the world human population, irrespective of gender and ethnicity (5, 23).

Peptide synthesis

Based on the bioinformatics analysis, 467 putative HLA-A*0201 binding peptides (9 mer long) from 84+ ORFs with high estimated half-times of dissociation ($T_{1/2}$) (Suppl. Table S1) were synthesized by Magenex (San Diego, CA) on a 9050 Peptide Synthesizer Instrument using solid-phase peptide synthesis and standard 9-fluorenylmethoxy carbonyl technology (PE Applied Biosystems, Foster City, CA). The purity of peptides was between 75 and 96%, as determined by reversed-phase high-performance liquid chromatography (Vydac C18) and mass spectroscopy (Voyager MALDI-TOF System). Stock solutions were made at 1 mg/ml in 10% DMSO in PBS. All peptides were aliquoted and stored at −20°C until assayed. Synthetic peptides corresponding to the 467 potential $CD8^+$ T cell epitopes, which belong to a total of 84^+ open reading frames (ORFs) encoded by the HSV-1 genome, were synthesized and then divided into 22 groups of peptides (Grp1 to Grp 22) (Suppl. Table S1). Each group of peptides contained an average of 20 peptides (range: 12 to 27 peptides) derived from 3 to 5 ORF proteins.

Binding with soluble HLA-A*0201 molecules

Quantitative assays to measure binding of each of 467 peptides to soluble HLA-A*0201 molecules are based on inhibition of binding of a radiolabeled standard peptide, as recently described (36). 1–10nM of radiolabeled peptide was co-incubated with 1μM–1nM purified MHC and 1–3μM human β2-microglobulin. After 2 days, binding of radiolabeled peptide to MHC class I molecules was determined by capturing MHC-peptide complexes on Greiner Lumitrac 600 micro plates coated with W6/32 antibody and measuring bond counts per minute using a Top count micro scintillation counter. Concentration of peptide yielding 50% inhibition of binding of radiolabeled probe peptide (IC_{50}) was then calculated (Suppl. Table S1).

Stabilization of HLA-A*0201 on class-I-HLA-transfected B × T hybrid cell lines (T_2 cell line)

To determine whether synthetic peptides could stabilize HLA-A*0201 molecule expression on the T_2 cell surface, peptide-inducing HLA-A*0201 up-regulation on T_2 cells was examined according to a previously described protocol (6). T_2 cells (3×10^5/well) were incubated with different concentrations of individual peptides in 48-well plates for 18 hours at 26°C. Cells were then incubated at 37°C for 3 hours in the presence of human β-2 microglobulin (1 μg/ml) and BD-Golgi stop (5 μg/ml), to block cell surface expression of newly synthesized HLA-A*0201 molecules. The cells were washed with FACS buffer (1% BSA and 0.1% sodium azide in 1X PBS) and stained with anti-HLA-A2.1 specific monoclonal antibody BB7.2 (BD-Pharmingen, USA) at 4°C for 30 min. After incubation, the cells were washed with FACS buffer, fixed with 2% PFA in 1X PBS, and analyzed by flow cytometry using a BD LSR II (Becton Dickinson, Mountain View, CA). The acquired data, including mean fluorescence intensity (MFI), were analyzed with a FlowJo software version 9.9.4 (TreeStar, Ashland, OR). Percent MFI increase was calculated as follows: Percent MFI increase = (MFI with the given peptide − MFI without peptide) / (MFI without peptide) × 100. Each experiment was performed 3 times, and means ± SD were calculated.

HLA-A2 typing

HLA-A2 sub-typing was performed using a commercial Sequence-Specific Primer (SSP) kit and following the manufacturer's instructions (SSPR1-A2; One Lambda, Canoga Park, CA). Genomic DNA extracted from PBMC of HSV-seropositive SYMP and ASYMP individuals was analyzed using a TECAN DNA workstation from a 96-well plate with 2μl volume per well, as we previously described (30). The yield and purity of each DNA sample was tested using a UV-spectrophotometer. The integrity of DNA samples was ascertained by electrophoresis on agarose gel. Each DNA sample was then subjected to multiple small volume PCR reactions using primers specific to areas of the genome surrounding the single point mutations associated with each allele. Only primers that matched the specific sequence of a particular allele would amplify a product. The PCR products were subsequently electrophoresed on a 2.5% agarose gel with ethidium bromide and the pattern of amplicon generation was analyzed using HLA Fusion Software (One Lambda, Inc., Canoga Park, CA). Additionally, the HLA-A2 status was confirmed by staining PBMC with anti-HLA-A2 mAb, BB7.2 (BD Pharmingen, USA), at 4°C for 30 min. The cells were washed, acquired on a BD LSR II, and analyzed using FlowJo software version 9.9.4 (TreeStar, Ashland, OR).

Peripheral blood mononuclear cell (PBMC) isolation

Individuals (negative for HIV, HBV, and with or without any HSV infection history) were recruited at UCI Institute for Clinical and Translational Science (ICTS). Between 40 and 100 mL of blood was drawn into yellow-top Vacutainer® Tubes (Becton Dickinson, USA). The serum was isolated and stored at −80°C for detection of anti-HSV-1 and HSV-2 antibodies, as we previously described (37). PBMC were isolated by gradient centrifugation using leukocyte separation medium (Cellgro, USA). The cells were washed in PBS and re-suspended in complete culture medium consisting of RPMI1640, 10% FBS (Bio-Products, Woodland, CA) supplemented with 1×penicillin/streptomycin/L-glutamine, 1× sodium pyruvate, 1× non-essential amino acids, and 50 μM of 2-mercaptoethanol (Life Technologies, Rockville, MD). Freshly isolated PBMC were also cryo-preserved in 90% FCS and 10% DMSO in liquid nitrogen for future testing.

Flow cytometry

For each stimulation condition, at least 500,000 total events were acquired on BD LSRII and data analysis was performed using FlowJo version 9.9.4 (TreeStar, Ashland, OR). PBMC were analyzed by flow cytometry after staining with fluorochrome-conjugated human specific monoclonal antibodies (mAbs). The following anti-human antibodies were used: CD3 (clone SK7) PE-Cy7, CD44 (clone G44-26) A700, CD8 (clone SK1) APC-Cy7, CCR7 (clone 150503) Alexa Flour 700, CD45RA FITC, CD62L APC, IFN-γ Alexa Fluor 647, $CD107^a$ (clone H4A3) FITC, $CD107^b$ (clone H4B4) FITC (BioLegend). The following anti-mouse antibodies were used to characterize mouse $CD8^+$ T_{CM}, $CD8^+$ T_{EM}, and $CD8^+$ T_{RM} sub-populations: anti-mouse CD8 (clone 53-6.7) PE-Cy7, anti-mouse CD44 (clone IM7) APC-Cy7, anti-mouse CD11a (clone M17/4) FITC, anti-mouse CD103 (clone M290) APC, anti-mouse CD62L (clone MEL-14) A700, anti-mouse CCR7 (clone 4B12) A647, anti-mouse CD69 (clone H1.2F3) PE-Cy7, $CD107^a$ (clone ID4B) FITC, $CD107^b$ (clone M3/84) FITC (BD Pharmingen), anti-mouse IFN-γ (clone XMG1.2) PE-Cy7, (Biolegend). TIGIT

(clone GIGD7) PE (eBiosciences), VISTA (clone 13f3, a gift from Dr. Noelle, Geisel School of Medicine at Dartmouth, Lebanon, NH). For surface stain mAbs against various cell markers were added to a total of 1×10^6 cells in 1X PBS containing 1% FBS and 0.1% sodium azide (FACS buffer) for 45 min at 4°C. After washing with FACS buffer, cells were permeabilized for 20 min on ice using the Cytofix/Cytoperm Kit (BD Biosciences) and then washed twice with Perm/Wash Buffer (BD Bioscience). Intracellular cytokine mAbs were then added to the cells and incubated for 45 min on ice in the dark. Cells were washed again with Perm/Wash and FACS Buffer and fixed in PBS containing 2% paraformaldehyde (Sigma-Aldrich, St. Louis, MO). For each sample, 200,000 total events were acquired on BD LSRII. Ab capture beads (BD Biosciences) were used as individual compensation tubes for each fluorophore in the experiment. To define positive and negative populations, we employed fluorescence minus controls for each fluorophore used in this study when initially developing staining protocols. In addition, we further optimized gating by examining known negative cell populations for background level expression. The gating strategy was similar to that used in our previous work (6). Briefly, we gated single cells, dump$^-$ cells, viable cells (Aqua Blue), lymphocytes, CD3$^+$ cells, and CD8$^+$ cells before finally gating human epitope-specific CD8$^+$ T cells using HSV-specific tetramers. Data analysis was performed using FlowJo version 9.9.4 (TreeStar, Ashland, OR). Statistical analyses were done using GraphPad Prism version 5 (La Jolla, CA).

Production of IFN-γ and expression of cytotoxic markers

To detect cytolytic CD8$^+$ T cells recognizing peptides in freshly isolated PBMCs we performed intracellular IFN-γ and CD107$^{a/b}$ cytotoxicity assay. Betts and colleagues have described the CD107$^{a/b}$ assay as an alternative cytotoxicity assay that is able to address some of the shortcomings of the ^{51}Cr release assay. The intracellular assay to detect IFN-γ and CD107$^{a/b}$ in response to *in vitro* peptide stimulations was performed as described (40, 42) with a few modifications. On the day of the assay, 1×10^6 PBMCs were stimulated *in vitro* with peptide pools (10μg/ml/peptide) at 37°C for additional 6 hrs in a 96-well plate with BD Golgi Stop (BD Biosciences), 10 μl of CD107^a FITC and CD107^b FITC. PHA (5μg/mL) (Sigma) and no peptide were used as positive and negative controls, respectively. At the end of the incubation period the cells were transferred to 96-well round bottom plate and washed twice with FACS buffer then stained with PE-conjugated anti-human CD8 for 45 min at 4°C. The intracellular staining for the detection of IFN-γ and CD107$^{a/b}$ was performed as outlined above. The cells were washed again and fixed, then 500,000 total events were acquired on BD LSRII and data analysis was performed using FlowJo version 9.9.4 (TreeStar, Ashland, OR). Peptide pools yielding positive responses were de-convoluted by testing individual peptides *in vitro* at 10μg/mL.

T-cell proliferation assay

CD8$^+$ T cell proliferation was measured using a CFSE assay as we recently described (5, 23). Briefly, PBMC were labeled with CFSE (2.5 μM, Molecular Probes) in 1X PBS at room temperature. Cold FCS was then added and cells were washed extensively with RPMI1640 plus 10% FCS. CFSE labeled cells were incubated with or without peptide pools and individual peptides (10μg/ml) and incubated for 6 days. As a positive control, 2 μg/ml of PHA was used to stimulate T cells for 3 days. The cells were then washed and stained with

PE-conjugated mAbs specific to human $CD8^+$ molecules. The numbers of dividing $CD8^+$ T cells per 300,000 total cells were analyzed by FACS. Their absolute number was calculated using the following formula: (# of events in $CD8^+/CFSE^+$ cells) × (# of events in gated lymphocytes) / (# of total events acquired).

Virus production

HSV-1 (strain McKrae) was used in this study (6) and was grown and titrated on rabbit skin (RS) cells. UV-inactivated HSV-1 was generated as we previously described (4). HSV inactivation was confirmed by the inability to produce plaques when tested on RS cells.

Design and construction of AAV8 vector expressing mouse chemokine under neurotropic promoters (CamKIIα and CMV)

The ORF for mouse chemokines (CCL5, CXCL9 or CXCL10) were cloned into SalI/EcoRI sites of pAAV-CamKIIα-MCS-CamKIIα-EGFP vector or pAAV-CMV-MCS-CMV-EGFP vector to determine the best vector for targeted delivery of chemokines in neuronal cells of mouse TG. These pAAV vectors were co-transfected with helper-plasmid in HEK293 cells to produce the AAV virus. 2 days after transfections, cell pellets were harvested, and viruses were released through 3 cycles of freeze/thaw. AAV viruses were purified through CsCl-gradient ultra-centrifugation, followed by desalting. Viral titers (GC/ml) were determined through real-time PCR.

Prime/pull therapeutic vaccine in “humanized” HLA-A*0201 transgenic mice

HLA-A*0201 transgenic mice were kindly provided by Dr. Lemonier (Pasteur Institute) and were recently described (1–3). To screen for neurotropic vector (CMV and CamKIIα), 6 – 8-week old HLA-A*0201 Tg mice were ocularly infected (without scarification of cornea) using 2×10^5 wild-type McKrae (HSV-1) strain. Thirty-five-days post-infection, when latency was fully established, reactivation of latent HSV-1 infection was induced following UV-B irradiation. Each eye was irradiated with 250 mJ of UV-B light/cm^2 (60 sec exposure on the transilluminator). Anesthetized mice were placed on the transilluminator – each mouse was positioned on a piece of cardboard containing a hole that is the same size as the mouse’s eye. This allowed just the eye to be irradiated by the UV-B source. Mice were divided into three groups for various days post UV-B irradiation (i.e. day 1, day 2, day 5, day 7 after UV-B exposure). Group 1 mice were administered AAV8-CamKIIα-mCXCL10-CamKIIα-eGFP vector. Group 2 mice were administered AAV8-CMV-mCXCL10-CMV-eGFP vector. Group 3 mice received an empty vector. Various days after chemokine administration, mice were sacrificed. The frequencies of $GFP^{(+)}NeuN^{(+)}$ neuronal cells were evaluated in TG of mice from all 3 groups.

For another experiment evaluating the prime/pull vaccine model, 6 to 8 weeks old HLA-A*0201 Tg mice were ocularly infected (without scarification of cornea) using 2×10^5 wild-type McKrae (HSV-1) strain. 21 days post-infection, when latency was fully established, mice were divided in three groups. Group 1 and group 2 were vaccinated with ASYMP epitopes selected from HSV-1 genome wide epitopes along with PADRE and CpG_{1826} adjuvant. Group 3 mice were mock vaccinated with CpG_{1826} adjuvant without ASYMP epitopes (mock vaccinated). After 2 weeks of vaccination (day 35 post infection), eyes of all

three groups of mice were UV-B exposed to induce virus reactivation. On day 37-post infection, the Group 2 mice received an additional treatment with 10^7 pfu of rAAV-8-CamKIIα-GFP-CamKIIα-CXCL10 vector (*vaccinated + CXCL10*). The virus shedding induced by UV-B exposure was quantified in eye swabs collected every day post UV-B light exposure (up to 10 days). Eyes were swabbed using moist, type 1 calcium alginate swabs that were then placed in 1.0 ml of titration media (Media 199, 2% penicillin/streptomycin, 2% newborn calf serum) and frozen at −80°C until titrated on RS cell monolayers as described previously (6). Animals were examined for signs of recurrent corneal herpetic disease by slit lamp for 30 days post UV-B, performed by investigators blinded to the treatment regimen of the mice and scored according to a standard 0 to 4 scale: 0, no disease; 1, 25%; 2, 50%; 3, 75%; and 4, 100% staining, as previously described (1–3). Following CXCL10 administration, mice were consequently sacrificed and the frequency and function of HSV-specific memory $CD8^+$ T cells were evaluated in TG of mice from all 3 groups. All animal experiments were conducted following NIH guidelines for housing and care of laboratory animals and were conducted in facilities approved by the University of California Irvine Association for Assessment and Accreditation of Laboratory Animal Care and according to Institutional Animal Care and Use Committee-approved animal protocols (IACUC # 2002–2372).

Immunohistochemistry

Mouse TG was cut into 8μm thick sections using a cryostat. Sections were washed with 1X PBS, permeabilized using 0.05% Triton-100X in 1X PBS for 15 min, and blocked using 10% FBS in 1X PBS for 1 hour. Sections were co-stained using anti-mouse mAbs specific to either A5 or KH10 neurons (1:200 dilution) and $CD8^+$ anti-rabbit antibody (1:200) overnight at 4°C. Sections were then washed with 1X PBS and co-stained with anti-mouse PE (1:500 indicating $A5^+$ or $KH10^+$ neurons) and Cy5 (1:200 indicating $CD8^+$ T cell proliferation). After secondary fluorescent staining, sections were washed with 1X PBS and mounted after DAPI staining (1:10000 dilution). Immunofluorescence localization of $A5^+$ or $KH10^+$ and $CD8^+$ with AAV8-GFP was examined using a Keyence BZ-X700 fluorescent microscope at 40X magnification and imaged using z-stack. (Blue: DAPI, Red: neuron ($A5^+$ or $KH10^+$), Green: AAV8, Yellow: CD8).

Statistical analysis

We examined the distribution of each immunological parameter. In the case of two group comparisons, we used the parametric two-sample *t*-test or non-parametric Wilcoxon rank sum test, as appropriate. For parameters satisfying a normal distribution, we used the F-test for equality of variances to determine if it would be appropriate to apply the Satterthwaite test assuming unequal variances between groups. For paired comparisons involving multiple peptides, we have used the conservative Bonferroni procedure to adjust for the 22 groups of peptides (Fig. 1), 22 or 23 individual peptides (Fig. 2), and four group comparisons (Fig. 4E, Fig. Suppl. Fig. S2) that were examined. We report the nominal *p*-values in the corresponding Figures after correction for multiple comparisons. In the specific case of three groups (i.e. comparing two subgroups with a baseline subgroup), we have used the General Linear Model procedure and compared the least squares means using the Dunnett procedure for multiple comparisons (Fig. 4B). Flow cytometry data were analyzed with FlowJo

software (TreeStar). For analysis, we used SAS® v.9.4 (Statistical Analysis System, Cary, NC). Graphs were prepared with GraphPad Prism software (San Diego, CA). Data are expressed as the mean + SD. Error bars show SEM.

RESULTS

Frequent HSV-specific IFN-γ-producing CD8$^+$ T cells, expressing cytotoxic markers, detected in seropositive individuals are directed against a limited number of epitopes from the HSV-1 genome

Peripheral blood mononuclear cells (PBMCs) from 20 HLA-A*0201$^{(+)}$ and 8 HLA-A*0201$^{(-)}$ HSV-seropositive individuals were stimulated *in vitro* for 72 hrs with each of the 22 groups of peptide epitopes (i.e. Grp.1 to Grp.22) spanning the entire HSV-1 genome. We then used intracellular FACS staining to measure IFN-γ and CD107$^{a/b}$ produced by stimulated CD8$^+$ T cells, as described in *Materials and Methods*.

Fig. 1A shows representative contour plots of percentages of IFN-γ$^+$CD8$^+$ T cells detected in one HLA-A*0201$^{(+)}$ and one HLA-A*0201$^{(-)}$ HSV-1 seropositive individual following stimulation with equimolar amounts of peptides from Grp.6, Grp.11 and Grp.16. Fig. 1B, shows average percentages of IFN-γ$^+$CD8$^+$ T cells detected from 20 HLA-A*0201$^{(+)}$ vs. 8 HLA-A*0201$^{(-)}$ HSV-1 seropositive individuals. The highest percentage IFN-γ$^+$CD8$^+$ T cells detected from 20 HLA-A*0201$^{(+)}$ HSV-1 seropositive individuals were directed against three groups of peptides: Grp.6, Grp.11 and Grp.16. The Grp.6 of HSV-1 peptides induced up to 4.4% IFN-γ$^+$CD8$^+$ T cells from 13 out of the 20 HLA-A*0201$^{(+)}$ HSV-1 seropositive individuals. Similarly, significant percentages of IFN-γ$^+$CD8$^+$ T cells (up to 6.6%) were detected in 17 out of 20 individuals in response to Grp.11 of HSV-1 peptides. The Grp.16 induced 1.6% to 3.9% of IFN-γ$^+$CD8$^+$ T cells in 15 out of 20 HSV-1 seropositive individuals. Grp.12 and Grp.20 induced a significant percentage of IFN-γ$^+$CD8$^+$ T cells in only 2 out of 20 HLA-A*0201$^{(+)}$ HSV-1 seropositive individuals. In contrast, none of the remaining 16 groups of HSV-1 peptides stimulated a significant percentage of IFN-γ$^+$CD8$^+$ T cells in any of the 20 HLA-A*0201$^{(+)}$ HSV-1 seropositive individuals tested. In parallel experiments, no significant percentages of IFN-γ$^+$CD8$^+$ T cells were detected from PBMC of the 8 HLA-A*0201$^{(-)}$ HSV-1 seropositive individuals when stimulated with equimolar amounts of the 22 groups of peptides, indicating the expected HLA specificity of the T cell responses. These results indicate that the HSV-1 peptides Grp.6, Grp.11, and Grp.16 contain at least one immunodominant IFN-γ-producing CD8$^+$ T cell epitope.

We next examined the ability of each group of HSV-1 peptides (i.e. Grp.1 to Grp.22) to induce cytotoxic CD8$^+$ T cells from 20 HLA-A*0201$^{(+)}$ and 8 HLA-A*0201$^{(-)}$ HSV-1 seropositive individuals. For this evaluation, we followed the expression of CD107^a and CD107^b on stimulated CD8$^+$ T cells by FACS and determined the percentage of CD107$^{a/b(+)}$CD8$^+$ T cells in HLA-A*0201$^{(+)}$ and HLA-A*0201$^{(-)}$ HSV-1 seropositive individuals. CD107^a and CD107^b are two markers of cytotoxic function, which are lysosomal-associated membrane glycoproteins that surround the core of the lytic granules in cytotoxic T lymphocytes (CTL). Upon TCR engagement and epitope stimulation, CD107$^{a/b}$ expression is upregulated on the cell membrane of CD8$^+$ cytotoxic T cells.

As shown in the representative data in Fig. 1C, Grp.6, Grp.11, and Grp.16 of HSV-1 peptides induced high percentages of $CD107^{a/b(+)}CD8^+$ T cells in PBMC from an HLA-A*0201$^{(+)}$ individual but not in PBMC from an HLA-A*0201$^{(-)}$ individual. Fig. 1D, shows average percentages of $CD107^{a/b(+)}CD8^+$ T cells detected from 20 HLA-A*0201$^{(+)}$ vs. 8 HLA-A*0201$^{(-)}$ HSV-1 seropositive individuals. The highest percentages of $CD107^{a/b(+)}CD8^+$ T cells detected from 20 HLA-A*0201$^{(+)}$ HSV-1 seropositive individuals was also directed against Grp.6, Grp.11 and Grp.16.

Up to 5.7% of $CD107^{a/b(+)}CD8^+$ T cells were recorded in PBMC from 16 out 20 HLA-A*0201$^{(+)}$ individuals following stimulation with HSV-1 peptides from Grp.6. Seventeen out of 20 HLA-A*0201$^{(+)}$ individuals responded strongly (up to 5.2%) to Grp.11 of peptides while 18 out of 20 HLA-A*0201$^{(+)}$ individuals showed up to 4.4% $CD107^{a/b+}CD8^+$ T cells in response to Grp.16 of peptides. The Grp.12 induced 2% to 3.6% of $CD107^{a/b(+)}CD8^+$ T cells in 8 out of 20 HLA-A*0201$^{(+)}$ individuals. Modest, yet significant percentages, of $CD107^{a/b(+)}CD8^+$ T cells were also detected against three additional groups of HSV-1 peptides: Grp.8, Grp.12 and Grp.20. In contrast, the remaining 13 groups of HSV-1 peptides did not induce significant percentages of $CD107^{a/b(+)}CD8^+$ T cells following stimulation of PBMC from 20 HLA-A*0201$^{(+)}$ HSV-1 seropositive individuals. As expected, none of 22 groups of HSV-1 peptides induced significant percentages of $CD107^{a/b(+)}CD8^+$ T cells in the 8 HLA-A*0201$^{(-)}$ HSV-seropositive individuals tested, indicating an HLA specificity in the cytotoxic $CD8^+$ T cell responses (Fig. 1D).

Because a lack of IFN-γ production and of $CD107^{a/b}$ expression may not always reflect a lack of T cell response (20, 38), we studied the proliferative response of $CD8^+$ T cells to the 22 groups of HSV-1 peptides from 20 HSV-1 seropositive individuals. PBMC were labeled with CFSE and then re-stimulated *in vitro* for six days with each of the 22 groups of HSV-1 peptides. As shown in Fig. 1E (*upper panel*), significant percentages of $CFSE^{low}CD8^+$ T cells were detected from one HLA-A*0201$^{(+)}$ individual when stimulated with Grp.6, Grp. 11, Grp.12 and Grp.16 of HSV-1 peptides. Grp.6, Grp.11, and Grp.16 induced the highest proliferation of $CD8^+$ T cells (30.2%, 32.5% and 35.7% of dividing $CFSE^{low}CD8^+$ T cells, respectively). Grp.12 induced a modest, yet significant, 11.8% of dividing $CFSE^{low}CD8^+$ T cells. In contrast, none of the remaining 18 groups of HSV-1 peptides induced significant proliferation of $CD8^+$ T cells in HLA-A*0201$^{(+)}$ individuals. No significant percentages of dividing $CFSE^{low}CD8^+$ T cells were induced by any 22 groups of HSV-1 peptides in HLA-A*0201$^{(-)}$ individuals, confirming the HLA specificity of the T cells responses (Fig. 1E, *lower panel*).

Altogether, these results indicate that Grp.6, Grp.11, and Grp.16 of HSV-1 peptides contain one or several immunodominant epitopes that induce HLA-A*020-restricted IFN-γ-producing $CD8^+$ T cells expressing cytotoxic markers in HLA-A*0201$^{(+)}$ HSV-seropositive individuals. Therefore, the remainder of this study focused on identifying the individual HSV-1 peptides from Grp.6, Grp.11, and Grp.16 that produced the $CD8^+$ T cell responses.

Immunodominant HSV-1 genome wide-derived epitopes targeted by IFN-γ-producing CD8+ T cells, expressing cytotoxic markers, from HLA-A*0201(+) HSV-seropositive individuals

We next compared the ability of individual HSV-1 peptides within Grp.6, Grp.11, and Grp. 16 groups to induce HSV-specific $CD8^+$ T cell responses in 10 HLA-A*0201$^{(+)}$ individuals vs. 8 HLA-A*0201$^{(-)}$ individuals.

As shown in the representative contour plots from Fig. 2A, 4.3% of IFN-γ^+CD8^+ T cells specific to the $UL9_{196–204}$ epitope were detected in an HLA-A*0201$^{(+)}$ while only 0.5% of IFN-γ^+CD8^+ T cells were detected in an HLA-A*0201$^{(-)}$ HSV-1 seropositive individual following stimulation with equimolar amount of the same peptide. Fig. 2B shows the average percentage of IFN-γ^+CD8^+ T cells detected in 10 HLA-A*0201$^{(+)}$ individuals as compared to 8 HLA-A*0201$^{(-)}$ individuals for each of the 23 individual peptides from Grp. 6. The highest percentage of IFN-γ^+CD8^+ T cells detected from 10 HLA-A*0201$^{(+)}$ HSV-1 seropositive individuals were directed against two immunodominant epitopes: the $UL9_{196–204}$ epitope (up to 4.1% of IFN-γ^+CD8^+ T cells) and the $UL10_{162–170}$ epitope (up to 4.3% of IFN-γ^+CD8^+ T cells). The $UL9_{196–204}$ epitope belongs to the HSV-1 replication-initiator UL9 protein and the $UL10_{162–170}$ belongs to the membrane UL10 protein. Fig. 2C shows representative contour plots of the percentage of IFN-γ^+CD8^+ T cells induced by the immunodominant $UL25_{572–580}$ epitope from Grp.11. Fig. 2D shows the average percentage of IFN-γ^+CD8^+ T cells detected in 10 HLA-A*0201$^{(+)}$ individuals vs. 8 HLA-A*0201$^{(-)}$ individuals for each of the 23 individual peptides from Grp.11. The highest % IFN-γ^+CD8^+ T cells were directed against three epitopes that belong to the HSV-1 DNA packaging tegument protein (UL25) and the capsid maturation protease (UL26): $UL25_{572–580}$ epitope (up to 3.7%), $UL26_{480–488}$ epitope (up to 4.0%) and $UL26_{(221–229)}$ epitope (up to 3.6%). Fig. 2E shows representative contour plots of % IFN-γ^+CD8^+ T cells induced by the immunodominant $UL43_{272–280}$ epitope from Grp.16. Fig. 2F shows the highest average % of IFN-γ^+CD8^+ T cells detected in 10 HLA-A*0201$^{(+)}$ individuals were directed mainly against six epitopes from Grp.16 that belong to the highly-conserved sequence in alpha- and gamma herpes virus envelope proteins UL43 and UL44: $UL43_{148–156}$ epitope (1.3% to 3.9%), $UL43_{272–280}$ epitope (2.3% to 6.2%), $UL43_{386–394}$ epitope (3.6% to 7.9%), $UL43_{302–310}$ epitope (3.1% to 7.0%), $UL44_{400–408}$ epitope (3.0% to 6.0%), and $UL44_{443–451}$ epitope (2.9% to 6.3%).

We then examined the ability of individual HSV-1 peptides from Grp.6, Grp.11, and Grp.16 to induce $CD8^+$ T cells expressing cytotoxic markers from 10 HLA-A*0201$^{(+)}$ and 8 HLA-A*0201$^{(-)}$ HSV-1 seropositive individuals. Fig. 2G shows the percentage of $CD107^{a/b+}CD8^+$ T cells specific to $UL9_{196–204}$ epitope from Grp.6 detected in one HLA-A*0201$^{(+)}$ and in one HLA-A*0201$^{(-)}$ HSV-1 seropositive individual. Fig. 2H shows the highest percentage $CD107^{a/b+}CD8^+$ T cells were detected in 10 HLA-A*0201$^{(+)}$ individuals were directed mainly against two UL9 and UL10 epitopes: $UL9_{196–204}$ (up to 5.1%) and peptide $UL10_{162–170}$ (up to 6.8%). Fig. 2I shows representative contour plots of % $CD107^{a/b+}CD8^+$ T cells detected in one HLA-A*0201$^{(+)}$ and one HLA-A*0201$^{(-)}$ HSV-1 seropositive individual following *in vitro* stimulation with the immunodominant peptide epitope $UL25_{572–580}$ from Grp.11. Fig. 2J shows that the average highest % $CD107^{a/b+}CD8^+$ T cells was detected against three epitopes from UL25 and UL26: $UL25_{367–375}$ (up to

2.5%), $UL25_{572–580}$ (up to 4.5%), and $UL26_{221–229}$ (up to 4.7%). Fig. 2K shows % $CD107^{a/b+}CD8^+$ T cells detected in one HLA-A*0201$^{(+)}$ and one HLA-A*0201$^{(−)}$ HSV-1 seropositive individual following *in vitro* stimulation with the immunodominant peptide epitope $UL43_{272–280}$ from Grp.16. Fig. 2L shows average highest % of $CD107^{a/b+}CD8^+$ T cells were detected against five peptide epitopes from UL43 and UL44: $UL43_{272–280}$ (up to 4.9%), $UL43_{386–394}$ (up to 5.2%), $UL43_{302–310}$ (up to 5.6%), $UL44_{400–408}$ (up to 5.7%), and $UL44_{443–451}$ (up to 5.1%). In parallel experiments, no significant percentage IFN-γ-producing $CD8^+$ T cells expressing cytotoxic markers were detected in 8 HLA-A*0201$^{(−)}$ HSV-1 seropositive individuals when stimulated with equimolar amounts of peptide epitopes from Grp.6, Grp.11, and Grp.16 (Figs. 2G to 2L), confirming the HLA specificity of the $CD8^+$ T cell responses.

Altogether, these results demonstrate that IFN-γ-producing $CD8^+$ T cells expressing cytotoxic markers in the majority of HLA-A*0201 positive HSV-1 seropositive individuals are directed against twelve epitopes derived from the whole HSV-1 genome: $UL9_{196–204}$, $UL10_{162–170}$, $UL25_{367–375}$, $UL25_{572–580}$, $UL26_{480–488}$, $UL26_{221–229}$, $UL43_{272–280}$, $UL43_{386–394}$, $UL43_{148–156}$, $UL43_{302–310}$, $UL44_{400–408}$, and $UL44_{443–451}$. Furthermore, we demonstrated that the 10 immunodominant epitopes above also induced significant $CD8^+$ T cell proliferative responses in the majority of HLA-A*0201 positive HSV-1 seropositive individuals (up to 32.4% of $CFSE^{Low}$ $CD8^+$ T cells) (Fig. S1). In contrast, a very low frequency of proliferative $CD8^+$ T cells (2.2% to 4.3% $CFSE^{Low}$ $CD8^+$ T cells) was detected from HLA-A*0201 negative controls in response to equimolar amounts of these individual peptides. These results confirm the immunodominance of the 12 epitopes from HSV-1 genome.

Most immunodominant HSV-1 genome-derived $CD8^+$ T cell epitopes bind with high affinity to, and stabilizes the expression of, HLA-A*0201 molecules on the surface of target cells

Ten potential epitopes with high predicted affinity to the HLA-A*0201 molecule were identified from the amino acid sequence of HSV1 genome (strain 17) using BIMAS, SYFPEITHI and MAPPP computational algorithms (Fig. 3A). We next assessed whether the 10 HSV-1 genome wide-derived $CD8^+$ epitopes predicted above would bind and stabilize HLA-A*0201 molecules on the surface of target cells. Binding affinities were determined in classical competition assays that measure the capacity of each peptide to competitively inhibit the binding of a high affinity radiolabeled reference Flu peptide to purified HLA-A*0201 molecules, as described in the *Methods* and in (36). The concentration of HSV-1 peptide yielding 50% inhibition of the binding of the radiolabeled reference peptide (IC_{50}) was calculated. Under the conditions utilized, the measured IC_{50} values are reasonable approximations of the true K_d values (39). As shown in Fig. 3B, 9 out of 10 HSV-1 genome wide-derived peptide epitopes bound with high affinity to soluble HLA-A*0201 molecules with an IC_{50} of less than 100nM. Notably, peptides, $UL25_{572–580}$, $UL26_{480–488}$, $UL26_{221–229}$ and $UL44_{400–408}$, bound with high affinity to HLA-A*0201 molecules with an IC_{50} of < 25nM. The $UL9_{196–204}$ peptide bound with high to intermediate binding affinities to HLA-A*0201 with an IC_{50} of ~46 nM. Peptides $UL10_{162–170}$, $UL43_{272–280}$, $UL43_{386–394}$ and $UL43_{302–310}$ bound with intermediate affinities to HLA-A*0201 with an IC_{50} between

>50nM and <100nM. The remaining $UL44_{443–451}$ peptide bound to HLA-A*0201 with low binding affinity (IC_{50} of 1099nM).

In an additional set of assays, we also determined the capacity of each peptide to stabilize the expression of HLA-A*0201 molecules on the surface of target T2 cells. As shown in Fig. 3C, 9 out of 10 peptides, $UL9_{196–204}$, $UL10_{162–170}$, $UL25_{572–580}$, $UL26_{480–488}$, $UL26_{221–229}$, $UL43_{386–394}$, $UL43_{302–310}$ and $UL44_{400–408}$ significantly increased the level of HLA-A*0201 molecules on the surface of T_2 cells as detectable by FACS, which suggest their high affinity for HLA-A*0201 molecules. The increase in HLA-A*0201 molecule expression was dose-dependent. The remaining $UL43_{272–280}$ and $UL44_{443–451}$ peptides demonstrated a moderate stabilization of HLA-A*0201 expression on the surface of T_2 cells, indicating their medium affinity for HLA-A*0201 molecules (Fig. 3C). Altogether, these results indicate that $UL9_{196–204}$, $UL10_{162–170}$, $UL25_{572–580}$, $UL26_{480–488}$, $UL26_{221–229}$, $UL43_{272–280}$, $UL43_{386–394}$, $UL43_{302–310}$, $UL44_{400–408}$, and $UL44_{443–451}$ bind with high to moderate affinity to HLA-A*0201 molecules and stabilize their expression on the surface of target cells.

Asymptomatic individuals have higher frequencies of multi-functional $CD8^+$ T_{EM} cells specific to HSV-1 genome wide-derived immunodominant epitopes while symptomatic individuals have higher frequencies of mono-functional $CD8^+$ T_{CM} cells

Next we investigated the frequency, phenotype, and function of HSV-1 genome-wide derived epitopes-specific $CD8^+$ T cells in HLA-A*0201$^{(+)}$ HSV-1 seropositive SYMP vs. ASYMP individuals (Table IA). SYMP individuals have frequent clinical ocular herpetic diseases, such as herpetic lid lesions, herpetic conjunctivitis, dendritic or geographic keratitis, stromal keratitis, and iritis consistent with recurrent HSK. This is in stark contrast to ASYMP individuals who, despite their HSV-1 seropositivity, have never had any recurrent herpes disease, ocular, genital or elsewhere, based on self-reporting and physician examination. The characteristics of the SYMP and ASYMP study populations used in the present study, with respect to gender, age, HLA-A*0201 frequency distribution, HSV-1/HSV-2 seropositivity, and status of ocular herpetic disease are presented in Table IB and detailed in the *Materials* and *Methods* section. Since HSV-1 is the main cause of ocular herpes, only individuals who were HSV-1 seropositive and HSV-2 seronegative were enrolled in the present study. The low frequencies of PBMC-derived HSV-specific $CD8^+$ T cells complicate a direct *ex vivo* tetramer detection of $CD8^+$ T cells using a typical number of PBMC (i.e. 1×10^6 cells), and a prior expansion of $CD8^+$ T cells by HSV-1 or peptide stimulation in an *in vitro* culture would hamper a reliable determination of the frequencies of HSV-1 epitopes-specific $CD8^+$ T cells. We therefore opted to determine the frequencies of HSV-1 epitopes-specific $CD8^+$ T cells *ex vivo* using a large number of PBMC ($\sim 10 \times 10^6$) per tetramer/CD8 mAb panel.

As shown in Fig. 4A (representative data) and Fig. 4B (average of frequencies), the highest and most significant frequencies of $CD8^+$ T cells detected in 8 SYMP and 8 ASYMP individuals were directed against 4 out of 10 peptide epitopes: $UL9_{196–204}$, $UL25_{572–580}$, $UL43_{302–310}$ and $UL44_{400–408}$ (1.7% to 5.9%). Interestingly, the average frequencies of $CD8^+$ T cells specific to $UL9_{196–204}$ epitope were consistently and significantly higher in HLA-A*0201$^{(+)}$ ASYMP individuals (Fig. 4B, *black circles*) as compared to HLA-

A*0201$^{(+)}$ SYMP individuals (Fig. 4B, *white circles*) ($P = 0.005$). In contrast, the average frequencies of CD8$^+$ T cells specific to UL43$_{302–310}$ epitope were significantly higher in HLA-A*0201$^{(+)}$ SYMP individuals as compared to HLA-A*0201$^{(+)}$ ASYMP individuals. The average frequencies of CD8$^+$ T cells specific to the remaining eight epitopes, UL10$_{162–170}$, UL25$_{572–580}$, UL26$_{480–488}$, UL26$_{221–229}$, UL43$_{272–280}$, UL43$_{386–394}$, UL44$_{400–408}$ and UL44$_{443–451}$, were at similarly low levels in both HLA-A*0201$^{(+)}$ SYMP and ASYMP individuals. The average frequencies of CD8$^+$ T cells specific to the 10 immunodominant epitopes in HLA-A*0201$^{(−)}$ controls did not yield any significant percentages, confirming the HLA specificity (Fig. 4B, *grey circles*).

CD8$^+$ T cells specific to the UL9$_{196–204}$ “ASYMP” epitope and to the UL43$_{302–310}$ “SYMP” epitope were visualized from SYMP and ASYMP individuals using ImageStream assay, as an alternative and complementary assay to FACS. Fig. 4C shows strong staining of CD8$^+$ T cells from one ASYMP individual when stained with a tetramer specific to the UL9$_{196–204}$ “ASYMP” epitope (*top left panel*) in contrast to a weak staining with a tetramer specific to the UL43$_{302–310}$ “SYMP” epitope (*top right panel*). Inversely, a strong staining of CD8$^+$ cells from one SYMP individual was detected when stained with a tetramer specific to the UL43$_{302–310}$ “SYMP” epitope (*bottom right panel*) in contrast to a weak staining with a tetramer specific to the UL9$_{196–204}$ “ASYMP” epitope (*bottom left panel*).

We next determined whether the memory CD8$^+$ T cells specific to the immunodominant UL9$_{196–204}$, UL25$_{572–580}$, UL43$_{302–310}$ and UL44$_{400–408}$ epitopes are composed of distinct sub-populations of central memory cells (i.e. CD44^{high}CD62^{high}CD8$^+$ T_{CM} cells) and effector memory cells (i.e. CD44^{high}CD62^{low}CD8 T_{EM} cells). As shown in Fig. 4D (representative data) and Fig. 4E (average of frequencies), ASYMP individuals had significantly higher percentages of CD44^{high}CC62L^{low}CD8$^+$ T_{EM} cells specific to UL9$_{196–204}$, UL25$_{572–580}$ and UL44$_{400–408}$ epitopes as compared to SYMP individuals ($P \leq 0.003$, unpaired *t*-Test). In contrast, significantly higher percentages of UL9$_{196–204}$ and UL25$_{572–580}$ epitope-specific CD8$^+$CD44^{high}CC62L^{high} T_{CM} cells were consistently detected in SYMP individuals as compared to ASYMP individuals ($P \leq 0.002$, unpaired *t*-Test).

Fig. 4F shows that overall 92% of ASYMP individuals had HSV-specific CD8$^+$ T_{EM} cells with 3 to 6 functions, indicating their ability to display concurrent polyfunctional activities: (*i*) production of high levels of IFN-γ; (*ii*) expression of high levels of cytotoxic markers (CD107$^{a/b}$/Perforin/GzmB) (Suppl. Fig. S2); (*iii*) proliferation; (*iv*) frequency of tetramer specific CD8$^+$ T cells; (*v*) stabilization of soluble HLA molecule: and (*iv*) T_2 binding assay. In contrast, only 42% of SYMP patients had HSV-specific CD8$^+$ T cells with 3 functions while the majority of them had just one or two functions.

Altogether, the frequency, phenotypic and functional properties of human CD8$^+$ T cells specific HSV-1 genome wide-derived epitopes suggest that: (*i*) some “ASYMP” epitopes (e.g. UL9$_{196–204}$) were associated with “natural” protection seen in ASYMP individuals. In contrast, other “SYMP” epitopes (e.g. UL43$_{302–310}$) were associated with a lack of protection seen in SYMP individuals; (*ii*) a clear dichotomy in HSV-specific memory CD8$^+$ T cell sub-populations exists in HSV-1 infected individuals, with ASYMP individuals

featuring higher frequencies of $CD8^+$ T_{EM} cells, while SYMP individuals featuring higher frequencies of $CD8^+$ T_{CM} cells; (*iii*) the majority of ASYMP individuals had multifunctional HSV-specific $CD8^+$ T_{EM} cells, with 3 to 6 functions, while the majority of SYMP individuals had mono-functional HSV-specific $CD8^+$ T_{CM} cells.

The above findings imply that following HSV-1 reactivation from latency, ASYMP individuals, but not SYMP individuals, would be better armed immunologically to control herpes infection and disease by mounting faster and stronger protective anti-viral $CD8^+$ T_{EM} cell responses. To test this hypothesis, throughout the remainder study, we will use our UV-B induced HSV reactivation mouse model (13, 14) to determine whether a therapeutic immunization of latently infected HLA-A*0201 transgenic mice (HLA-A*0201 Tg mice) with "ASYMP" epitopes will preferentially induce HSV-specific T_{EM} cells associated with protection against recurrent herpes.

Successful delivery of CXCL10 chemokine to HSV-1 latently infected trigeminal ganglia using the neurotropic recombinant non-replicating adeno-associated virus type 8 (AAV8) vector

We next investigated whether a chemokine-encoding recombinant replication deficient AAV8 vector, that preferentially infects the neurons: (*i*) would deliver the T-cell attracting chemokines CCL5, CXCL9 and CXCL10 into HSV-1 latently infected trigeminal ganglia (TG); and (*ii*) whether that would be accompanied with an increase in the number of $CD8^+$ T cells infiltrating TG.

To optimize such delivery, we first searched for a promoter that would lead to a specific and optimal expression of a green fluorescent protein (GFP) in sensory neurons of HSV-1 latently infected TG. Two types of promoters were tested: (1) the universal CMV promoter; and (2) the neurotropic CamKIIα-promoter. The CMV or CamKIIα promoters were used to control expression of both GFP and CXCL10 chemokine resulting in two different types of AAV8 vectors: the rAAV8-CMV-GFP-CMV-CXCL10; and (2) the rAAV8-CamKIIα-GFP-CamKIIα-CXCL10 vector (Fig. 5A).

A group of HLA-A*0201 Tg mice ($n = 30$) latently infected with HSV-1 were exposed to UV-B on day 35 post-infection (PI) to induce HSV-1 reactivation. The mice were then divided into three groups ($n = 10$/group) and on day 37 PI, received topical ocular application of 10^7 pfu of: (1) the rAAV8-CMV-GFP-CMV-CXCL10; (2) the rAAV8-CamKIIα-GFP-CamKIIα-CXCL10 vector; or (3) an empty AAV8 vector as control. The percentages of $NeuN^{(+)}$ neuronal cells expressing GFP (i.e. $NeuN^{(+)}GFP^{(+)}$) were determined from total cells isolated from TG by FACS at various days post-inoculation.

As shown in Fig. 5B (*left panel*, representative data and r*ight panel* average of frequencies), six days following topical ocular application of rAAV8-CamKIIα-GFP-CamKIIα-CXCL10, 27.1% to 39.4% of $GFP^{(+)}NeuN^{(+)}$ neuronal cells in TG of HLA-A*0201 Tg mice expressed GFP. In contrast, only about half (~14.5 %) of $GFP^{(+)}NeuN^{(+)}$ neuronal cells in TG expressed GFP following a topical ocular application of the rAAV8-CMV-GFP-CMV-CXCL10 vector ($P < 0.05$). The expression of GFP in TG persists for at least 3 wks. (not shown). As expected, no significant percentage of $GFP^{(+)}NeuN^{(+)}$ neuronal cells was

detected in control TG that received the empty AAV8 vector. These results indicate that the neurotropic CamKIIα is an optimal promoter for expression of T cell-attracting chemokines in HSV-1 latently infected TG.

Using the optimal CamKIIα promoter, we then constructed two additional rAAV8 vectors expressing the remaining T-cell attracting chemokines: CCL5 and CXCL9 (in addition to CXCL10) (Fig. 5C): (1) rAAV8-CamKIIα-GFP-CamKIIα-CCL5; and (2) rAAV8-CamKIIα-GFP-CamKIIα-CXCL9. We next determined which one of the three chemokine-encoding recombinant non-replicating AAV8 vectors shown in Fig. 5C would recruit more $CD8^+$ T cells in HSV-1 latently infected TG. Three groups of HSV-1 latently infected HLA-A*0201 Tg mice ($n = 30$/group) were treated with UV-B on day 35 PI to induce HSV-1 reactivation and 2 days later were inoculated with: (1) the rAAV8-CamKIIα-GFP-CamKIIα-CCL5; (2) the rAAV8-CamKIIα-GFP-CamKIIα-CXCL9; or (3) the rAAV8-CamKIIα-GFP-CamKIIα-CXCL10 vector (Fig. 5D). An empty AAV8 vector was used as control. The percentages of $GFP^{(+)}NeuN^{(+)}$ neuronal cells as well as the percentages $CD103^+CD8^+$ T cells were determined in TG cell suspension using FACS assay. As shown in Fig. 5E, inoculation of the rAAV8-CamKIIα-GFP-CamKIIα-CXCL10 vector led to significantly more $CD8^+$ T cells in TG of latently infected HLA-A*0201 Tg mice compared to rAAV8-CamKIIα-GFP-CamKIIα-CCL5 and rAAV8-CamKIIα-GFP-CamKIIα-CXCL9 vectors ($P < 0.05$). Similar percentages of $GFP^{(+)}NeuN^{(+)}$ neuronal cells were detected in TG of latently infected HLA-A*0201 Tg mice for all three vectors indicating that similar level of chemokines was expressed (not shown). No corneal pathology or recurrent HSK associated with any of the three chemokine-encoding recombinant non-replicating AAV8 vectors. Interestingly, GFP appeared to be expressed almost exclusively in $KH10^{(+)}$ neurons, but not in $A5^{(+)}$ neurons (Fig. 5F, *top two panels*). As a result, more $CD8^+$ T cells were located around $KH10^{(+)}$ neurons than $A5^{(+)}$ neurons (Fig. 5F, *bottom two panels*).

Altogether, these results indicate that: (*i*) the neurotropic CamKIIα promoter, but not the CMV promoter, is optimal for T-cell attracting chemokines expression in HSV-1 latently infected TG; (*ii*) inoculation of the rAAV8-CamKIIα-GFP-CamKIIα-CXCL10 vector led to significant more $CD8^+$ T cells in TG of latently infected HLA-A*0201 Tg mice as compared to the rAAV8-CamKIIα-GFP-CamKIIα-CCL5 and rAAV8-CamKIIα-GFP-CamKIIα-CXCL9 vectors; and (*iii*) GFP and CXCL10 chemokine under the neurotropic CamKIIα promoter appeared to be highly expressed in $KH10^{(+)}$ neurons, but not in $A5^{(+)}$ neurons.

Bolstering the number and function of HSV-specific $CD8^+$ T cells in latently infected TG through a prime/pull therapeutic vaccine

We next determined whether priming with multiple HSV-1 “ASYMP” human $CD8^+$ T cell epitopes followed by topical ocular treatment with the rAAV8-CamKIIα-GFP-CamKIIα-CXCL10 vector would: (*i*) pull more functional anti-viral $CD8^+$ T cells within HSV-1 latently infected TG; and (*ii*) provide protective immunity at the site of virus reactivation (i.e. HSV-1 latently infected TG) associated with reduced virus shedding and recurrent ocular herpes following UV-B induced reactivation.

As shown in Fig. 6A, thirty HLA-A*0201 Tg mice ($n = 30$) were ocularly infected with HSV-1 and twenty-one days post-infection, when latency was fully established, mice were

divided in three groups (n = 10/group). Groups 1 and 2 received a subcutaneous immunization on day 21 with the three HSV-1 "ASYMP" $CD8^+$ T cell epitopes ($UL9_{196–204}$, $UL25_{572–580}$ and $UL44_{400–408}$) associated with "natural" protection seen in ASYMP individuals, mixed with the promiscuous $CD4^+$ T helper epitope PADRE and CpG_{1826} adjuvant. Group 3 served as a negative control and received adjuvant alone (*mock vaccinated*). Two-weeks post-vaccination (i.e. on day 35 post infection), all animals were exposed to UV-B light in order to induce HSV-1 reactivation, as we recently described (13, 14). On day 37 post-infection, Group 2 received an additional treatment with 10^7 pfu of the rAAV8-CamKIIα-GFP-CamKIIα-CXCL10 vector (*vaccinated + CXCL10*), as above.

Eye swabs were collected every day post UV-B light exposure (up to 10 days) and recurrent corneal herpetic disease was recorded for 30 days and scored on the scale of 0–4, as described in *Materials & Methods*. As shown in Figs. 6B and 6C, 4 mice from the "*vaccinated + CXCL10*" group have no disease (score 0), 5 mice have a minor disease (score of 1), while only one mouse has a score of 3. In contrast, 2 mice from the "*vaccinated*" group, which did not receive CXCL10 treatment had minor disease (score 1), 6 mice have a disease score of 2, while two mice have a score of 4. As expected, most mice from the "*mock-vaccinated*" group had notable recurrent herpetic disease with a score of 3 to 4. Additionally, we recorded significantly low virus titers from mice that were both vaccinated and CXCL10 treated as compared to mice that were only vaccinated and to mock-vaccinated mice (P = 0.01, Fig. 6D). These results suggest that the prime/pull vaccine based on "ASYMP" epitopes and CXCL10 did improve protection against virus shedding and recurrent disease.

Representative FACS plots (Fig. 6E), average frequencies (Fig. 6F) and absolute numbers (Fig. 6G) of ASYMP $UL9_{196–204}$ epitope-specific functional $CD8^+$ T cells were determined in TG. Significantly higher frequencies of: (*i*) HSV-specific IFN-γ^+CD8^+T cells; and (*ii*) HSV-specific $CD107^{a/b(+)}CD8^+$T cells; and significantly lower frequencies of (*iii*) HSV-specific PD-$1^{(+)}CD8^+$ T cells and (*iv*) HSV-specific $VISTA^{(+)}CD8^+$T cells were detected in TG of mice that were vaccinated and treated with CXCL10 as compared to mice that received the vaccine alone (P = 0.02) indicating that CXCL10 chemokine treatment contributed to increased function of TG-resident HSV-specific T cells.

Furthermore, there was a positive correlation between the percentage (Fig. 7A) and the numbers (Fig. 7B) of $CD8^+$ T cells in TG of HLA-A*0201 Tg mice and protection against recurrent disease, indicating a $CD8^+$ T cell-dependent protective mechanism. This suggests that local encounters with HSV-1 antigen are critical for activation of TG-resident $CD8^+$ T cells. The effect of prime/pull therapeutic vaccine persisted for at least 4 weeks and occurred only in mice that were exposed to UV-B reactivation (not shown).

To identify the $CD8^+$ T cell sub-populations (i.e. T_{RM}, T_{CM}, T_{EM}) that correlated with protection in a final group of experiments, 30 mice were infected, divided in three groups, vaccinated, and exposed to UV-B, as shown in Fig. 6A above. Single cell suspension was obtained from TGs and stained for markers of $CD8^+$ T_{RM}, T_{CM} and T_{EM} cells including CD8, CD11a, CD69, CD103, CD44, CD62L, and CCR7 and analyzed by FACS. Significantly higher frequencies (Figs. 7C and 7D) and absolute numbers (Fig. 7E) of

ASYMP $UL9_{196–204}$ epitope-specific $CD8^+$ T_{RM} cells (*top panels*), $CD8^+$ T_{CM} cells (*middle panels*), and $CD8^+$ T_{EM} cells (*bottom panels*) were detected in TG of mice that were vaccinated compared to mice that were both vaccinated and treated with CXCL10 ($P < 0.05$). The frequency of $UL9_{196–204}$ epitope-specific $CD8^+$ T_{EM} cells doubled in TG of protected HLA-A*0201 Tg mice that were vaccinated and treated with CXCL10 (i.e. 6.1% vs. 14.9%, respectively). In contrast, no significant difference in the frequency of $CD8^+$ T_{CM} cells was detected in TG of mice that were vaccinated compared to mice that were both vaccinated and treated with CXCL10 ($P > 0.05$ *middle panels*). Expansion of T_{RM} and T_{EM} occurs only in mice that were exposed to UV-B reactivation (not shown). This confirms that local exposure to HSV-1 antigens is critical for expansion of these TG-resident $CD8^+$ T cell sub-populations

These results (*i*) demonstrate that bolstering the number of functional HSV-specific $CD8^+$ T_{EM}, and T_{RM} cells in TG of latently infected HLA-A*0201 Tg mice reduced viral shedding in tears and recurrent ocular herpetic disease following UV-B light induced reactivation; and (*ii*) suggest that protective anti-viral $CD8^+$ T cell population in latently infected TG is not compartmentalized only into tissue-resident T_{RM} cell sub-population, but can also be replenished by the $CD8^+$ T_{EM} cell sub-population that can migrate from circulation.

DISCUSSION

HSV-specific $CD8^+$ T cells that reside in latently infected trigeminal ganglia appeared to play a critical role in aborting attempts of HSV-1 reactivation from sensory neurons (23, 30). In designing a human herpes therapeutic vaccine, it is critical to identify the protective herpes epitopes derived from the 84^+ ORFs of HSV-1 genome, which are exclusively recognized by the human $CD8^+$ T cells from “naturally” protected ASYMP individuals who, despite being infected they never develop any recurrent herpetic disease. In the present study, we have implemented several *in silico, ex vivo, in vitro*, and *in vivo* phenotypic and functional immunological methods to efficiently generate a genome-wide map of the responsiveness of HSV-specific $CD8^+$ T cells in ASYMP individuals. This leads to identification of several previously unknown protective human “ASYMP” $CD8^+$ T cell epitopes. These “ASYMP” epitopes are associated with frequent, robust, and polyfunctional $CD8^+$ T_{EM} cell responses. Moreover, therapeutic immunization of a novel susceptible “humanized” HLA-A*0201 Tg mouse model with “ASYMP” epitopes induced a strong $CD8^+$ T cell-dependent protective immunity against recurrent ocular herpes. Furthermore, we report a novel prime-pull therapeutic vaccine strategy, based on priming $CD8^+$ T cells with multiple “ASYMP” epitopes followed by treatment with the CXCL10 T cell-attracting chemokine. This approach significantly boosts the number of functional anti-viral $CD8^+$ T_{EM} and T_{RM} cells in TG of HSV-1 latently infected humanized” HLA Tg mice and improves protection against recurrent herpetic disease following UV-B induced HSV-1 reactivation. These findings have profound implications in the development of T-cell-based immunotherapeutic vaccine strategies to treat recurrent herpes infection and disease in man.

Development of $CD8^+$ T cell epitope-based vaccines in the era of omics is taking advantage of new technologies to tackle infectious diseases for which vaccine development has been unsuccessful (12). Cutting-edge technologies and screening strategies have been developed

recently to mine genomic sequence information for state-of-the-art rational vaccine design (40). However, the large size of the HSV-1 genome and the low frequency of HSV-specific $CD8^+$ T cells have hampered genome-wide identification of protective HSV-1 $CD8^+$ T cell epitopes and characterization of the full repertoire of $CD8^+$ T cells that are associated with the “natural protective immunity" seen in ASYMP individuals. The HSV-1 genome is a linear double-stranded DNA sequence of approximately 152 Kb and contains two unique regions called the long unique region (UL) and the short unique region (US), which together encode 84^+ open reading frames (ORFs) (41). Recent availability of comprehensive genomic datasets of HSV-1 has shifted the paradigm of herpes vaccine development from virological to sequence-based approaches (41). Our genome-wide screening of the HSV-1 sequence using cohorts of SYMP and ASYMP individuals identified several previously unknown $CD8^+$ T cell epitopes that span a wide range of envelope, structural, and tegument HSV-1 proteins. We have characterized the phenotype and function of $CD8^+$ T cell epitopes both in ASYMP humans and in HLA-A*0201 Tg mice. Importantly, an innovative prime/pull therapeutic vaccine strategy that increases the size and function of HSV-specific $CD8^+$ T cell in latently infected TG has been demonstrated for the first time in a “humanized” animal model of recurrent ocular herpes. Thus, our novel vaccination strategy has produced scores of new protective “ASYMP” $CD8^+$ T cell epitopes as well as an innovative delivery system that is prime for clinical trial testing.

One of the advantages of ASYMP epitope-based vaccines, as opposed to protein-based vaccines, is the avoidance of SYMP epitopes that might inadvertently drive unwanted immuno-pathological responses (42). Such immuno-pathological responses might contribute to exacerbation of disease as recently found for an HLA-A*0201-restricted $CD8^+$ T cell epitope from the HSV-1 gK protein (43). Thus, identification of human “SYMP” epitopes from the HSV-1 genome and their elimination from a therapeutic herpes vaccine would be beneficial, since “SYMP” epitopes may be harmful by exacerbating recurrent herpetic disease.

HSV-1 expresses its genes sequentially in four kinetic classes of proteins: (*i*) the immediate early α (most of which are transcriptional factors); (*ii*) the early β (mostly enzymes); (*iii*) the early late γ1 (mostly of which are structural proteins); and (*iv*) the true late γ2 (mostly structural proteins and viral particles). The repertoire of HSV-specific $CD8^+$ T cells typically targets epitopes from only a fraction of the viral proteins. Those viral epitopes usually fall into a dominance hierarchy consisting of one or few dominant epitopes and several other sub-dominant epitopes. Most studies of HSV-specific $CD8^+$ T cells in animal models, including ours, use C57BL/6 mice (44, 45). A genome-wide approach was recently used to predict 376 potential HSV-1 $CD8^+$ T cell epitopes in HSV-1 infected C57BL/6 mice (46, 47). Functional $CD8^+$ T cells in HSV-1 infected C57BL/6 mice actually target only 19 out of the 376 potential epitopes (46, 47). These 19 epitopes identified virtually all or the vast majority of the HSV-specific mouse $CD8^+$ TCR repertoire. The 19 mouse HSV-1 epitopes are derived from only 11 of 84^+ HSV-1 proteins (46, 47). Of the four kinetic classes of HSV proteins, no immediate early α gene products are targeted by mouse $CD8^+$ T cells, 11 of 19 epitopes are derived from four early β gene products, 4 of 19 epitopes are derived from one early late γ1 gene product, and the remaining 4 epitopes are from four true late γ2 gene products that require viral DNA synthesis (46, 47). Strikingly, an incredible 50% to 70% of

all HSV-specific $CD8^+$ T cells in infected C57BL6 mice target a single glycoprotein B immuno-dominant epitope: $gB_{498–505}$. Through the use of a similar genome-wide comprehensive approach in this study, we identified several new human $CD8^+$ T cell epitopes from HSV-1 proteins not previously considered as vaccine candidates. In contrast to mouse $CD8^+$ T cells, human HSV-specific $CD8^+$ T cells targeted each of the four kinetic classes of HSV proteins (i.e. α, β, γ1 and γ2) (48, 49). These targets include epitopes from four immediate early α gene products, four early β gene products, and four early late γ1 gene products, while the remaining seven are from γ2 gene products (48, 49). Thus, unlike in C57BL/6 mice, the human $CD8^+$ T cell epitopes are derived from viral proteins that are produced both before and after viral DNA synthesis. It seems clear that the HSV-specific $CD8^+$ T cell repertoire detected in C57BL6 mice during acute infection does not reliably represent the human $CD8^+$ T cell repertoire (24).

The complexity of the $CD8^+$ T cell responses ranged from 3 to 20 reactive ORF/HLA combinations per ASYMP individual. We found that most immunodominant human epitopes derived from the whole HSV-1 genome: $UL9_{196–204}$, $UL10_{162–170}$, $UL25_{367–375}$, $UL25_{572–580}$, $UL26_{480–488}$, $UL26_{221–229}$, $UL43_{272–280}$, $UL43_{386–394}$, $UL43_{148–156}$, $UL43_{302–310}$, $UL44_{400–408}$, and $UL44_{443–451}$ are from Long Unique region (UL) of the HSV genome. Out of 12 immunodominant epitopes, 3 epitopes were from the early stage of HSV-1 replication ($UL9_{(196–204)}$, $UL26_{(480–488)}$ and $UL26_{(221–229)}$) while 9 epitopes ($UL10_{(162–170)}$, $UL25_{(367–375)}$, $UL25_{(572–580)}$, $UL43_{(148–156)}$, $UL43_{(272–280)}$, $UL43_{(386–394)}$, $UL43_{(302–310)}$, $UL44_{(400–408)}$ and $UL44_{(443–451)}$) were from the late stage of assembly and replication of HSV-1. It has been proposed that the most important T cell epitopes in HSV may be in tegument or other non-capsid proteins (50, 51). Tegument proteins, such as those encoded by UL41, UL46/VP11/12, UL47/VP13/14, UL48/VP16, and UL49, as well as immediate early (IE) proteins including RL2/ICP0 and RS1/ICP4 are major targets for effector T cells (50, 51).

Overall, based on our own and others' results, unlike the mouse HSV-specific $CD8^+$ T cell repertoire in the aforementioned mouse studies, the human HSV-specific $CD8^+$ T cell repertoire appear to target a much wider range of 20 out of 84^+ HSV proteins (48, 49). Interestingly, HSV-specific $CD8^+$ T cells from both mice and humans are commonly directed against 5 of the 84^+ HSV proteins. However, human $CD8^+$ T cell dominance hierarchy is also different from that of mice since no human $CD8^+$ T cell immuno-dominant epitope equivalent to the HSV $gB_{498–505}$ has been reported in humans. In contrast, the epitopes recognized by human $CD8^+$ T cells appeared to be evenly distributed between the 20 HSV-1 proteins (48, 49). These differences in the array, dominance, and hierarchy of HSV proteins targeted by human and mouse HSV-specific $CD8^+$ T cells make the reliability of C57BL/6-HSV model to the human-HSV host-pathogen "natural" combination questionable (24). The distribution and the profile of HSV-specific $CD8^+$ T cell responses detected in the C57BL/6-HSV mouse model appears to be "artificially" uneven (52). This unusual distribution of $CD8^+$ T cell responses does not reflect the $CD8^+$ T cell profile of responses we, and others (48, 49) have detected in the human-HSV host-pathogen "natural" combination.

After primary infection of epithelial surfaces, the alpha-herpesviruses, such as HSV-1, often establish latent infection in the sensory neurons of their natural hosts (34, 53). During this process, antiviral memory $CD8^+$ T cells develop and co-exist for years along with latent HSV-1 (27, 34, 53). Sufficient numbers of functional memory $CD8^+$ T cells in TG of ASYMP individuals are critical for suppressing (or aborting) attempts of virus reactivation from latency (34). However, the apparent feeble numbers of existing memory $CD8^+$ T cells in TG of SYMP individuals might not be sufficient to eliminate virus reactivation and would result in the observed repetitive symptomatic shedding and recurrent herpetic disease (23, 30). Therapeutic vaccines can be designed to enhance the existing memory $CD8^+$ T cell sub-populations in TG for increased protection against virus reactivation and hence eliminate or reduce re-infection of the cornea and recurrent herpetic disease. Boosting the apparent feeble numbers of functional memory $CD8^+$ T_{EM} cells that we detected in SYMP individuals may also contribute in reducing HSV-1 reservoir in latently infected TG. Consequently, this would actively suppress or permanently silence virus reactivation that occurs in latently infected sensory neurons of TG thus stopping or reducing recurrent disease. However, the relative contribution of tissue-resident, peripheral and recirculating memory $CD8^+$ T cells (i.e. T_{CM}, T_{RM}, T_{RM}) in protection against recurrent herpes infection and disease remains to be fully elucidated. In the present pre-clinical study, we demonstrate that a novel prime/pull therapeutic vaccine strategy, consisting of priming antiviral $CD8^+$ T cells with “ASYMP” human epitopes followed by neurotropic CXCL10 treatment, can bolster the number and broaden the repertoire of functional antiviral $CD8^+$ T_{EM} and T_{RM} cells, but not of $CD8^+$ T_{CM} cells, in TG of latently infected HLA-A*0201 Tg mice. This boost was associated with a significant reduction in viral shedding and recurrent ocular herpetic disease following UV-B induced reactivation. This finding suggest that: (*i*) both tissue-resident T_{RM} cells and recirculating effector memory T_{RM} cells contribute greatly to protection against recurrent herpes infection and disease; and (*ii*) $CD8^+$ T_{EM} cells in latently infected TG can be replenished from an apparent recruitment from the blood, provided that appropriate T-cell attracting chemokines, such as CXCL10, are delivered locally into TG. Additionally, T_{RM} cells likely expand locally following encounter with reactivated virus and viral antigen in sensory neurons. These findings further confirm our hypothesis that HSV-1 latency/reactivation cycle occurring in sensory neurons might be eliminated or permanently silenced if sufficient numbers of functional HSV-specific $CD8^+$ T_{EM} and T_{RM} cells can be mobilized into latently infected TG by a prime/pull therapeutic vaccine.

In the present study, frequent effector memory IFN-$\gamma^+$$CD107^{a/b+}$$CD44^{high}$$CD62L^{low}$$CD8^+$ T_{EM} cells specific to HSV-1 genome-derived epitopes were detected in ASYMP individuals. In contrast, $CD8^+$ T cells in SYMP individuals predominantly consisted of central memory $CD44^{high}CD62L^{high}CD8^+$ T_{CM} cells. This is consistent with our previous findings of significantly higher proportions of $CD8^+$ T_{EM} cells specific to epitopes from gB (32), from VP11/12 (15), and from VP13/14 (54) in ASYMP individuals. Though we are aware that information gained from PBMC-derived T cells may not be completely reflective of TG-resident $CD8^+$ T cells, our investigations were limited to human PBMC-derived $CD8^+$ T cells because of the ethical and practical challenges in obtaining human TG-resident $CD8^+$ T cells. Nevertheless, both the human and mouse results converge into suggesting that ASYMP individuals mount faster and stronger poly-functional HSV-specific $CD8^+$ T_{EM} and

$CD8^+$ T_{RM} cell responses that allow for a fast and better clearance of herpes reactivation and recurrent disease.

The inadequacy of many animal models of herpes infection and immunity have made it challenging to explore the immune mechanisms that lead to protection against recurrent herpetic disease (17). A critical question is which animal model would be the most appropriate to mimic the immuno-pathological aspects of recurrent herpetic disease as occurs in humans? Mice have been the animal models of choice for most herpes immunologists and the results from mouse models have yielded tremendous insights into the protective mechanisms during primary acute infection (reviewed in (19)). Characterization of the phenotype and function of protective HSV-specific memory $CD8^+$ T cells in mice have been largely limited to T cells specific to the immunodominant HSV-1 $gB_{495–505}$ epitope studied during acute infection (35, 46). Unlike humans, spontaneous HSV-1 reactivation in latently infected mice and virus shedding in tear film either does not occur at all or occurs at very low levels in mice (55). Thus, despite evidence that the majority of clinical recurrent HSK is due to reactivation (42, 56), most pre-clinical animal studies investigating the mechanisms that orchestrate recurrent HSK have used primary acute infection of mice (57, 58). Only a handful of studies have employed the mouse model of UV-B light induced recurrent herpetic corneal disease, mostly using C57BL/6 and BALB/c mice (59–61). Moreover, considering the wealth of data addressing the protective mechanisms of $CD8^+$ T cells specific to mouse HSV-1 epitopes (mostly in acutely infected C57BL/6), it is surprising how few reports exist exploring the protective mechanisms of $CD8^+$ T cells specific to human HSV-1 epitopes (59, 61). The present study validated the UV-B light induced recurrent herpetic corneal disease in the “humanized” HLA Tg mouse model of ocular herpes (4, 30). The study showed that both shedding of reactivated virus in tears and recurrent corneal HSV can be induced by UV-B exposure of latently infected HLA Tg mice. Moreover, our “humanized” HLA Tg mice express the human HLA-A*0201 molecule, instead of mouse $H2^b$ or $H2^d$ MHC molecules. Thus, they develop “human-like” $CD8^+$ T-cell responses to HLA-restricted epitopes (62). In addition, after UV-B induced reactivation, high numbers of functional $CD8^+$ T_{RM} and T_{EM} cells were detected in TG and were associated with protection against induced recurrent herpetic disease. In contrast, high number of exhausted $CD8^+$ T-cells in TG are associated with severe recurrent disease in these mice. Until recently, it was not possible to directly evaluate therapeutic vaccine efficacy of human HLA-restricted $CD8^+$ T cell epitopes in a small animal model of recurrent ocular herpes. In our opinion, the HLA Tg mice combined with UV-B induced recurrent disease is arguably the best available small animal model to study the role of HLA-restricted $CD8^+$ T-cells specific to human HSV-1 epitopes in protection against virus shedding and recurrent herpetic disease. Ongoing studies in our laboratory are using the HLA Tg mouse model of UV-B induced recurrent disease to investigate the dynamics of both TG- and cornea-resident antiviral $CD8^+$ T cells that may lead to SYMP vs. ASYMP infections.

Following acute infection, three major HSV-specific memory $CD8^+$ T cell sub-populations, T_{CM}, T_{EM} and T_{RM}, develop, infiltrate and sequester in the infected TG in response to a high level of T cell-attracting CXCL9, CXCL10 and CCL5 chemokines and other factors early during acute infection (1, 15, 32). Memory $CD8^+$ T cell infiltrates were reported in latently infected TGs of human cadavers (63). Functional $CD8^+$ T cells in these infiltrates

likely help decrease viral shedding by aborting attempts of virus reactivation from latency (23, 30). However, the apparent low level of T cell-attracting CXCL9, CXCL10 and CCL5 chemokines in latently infected TG may not be sufficient to control sequestration of $CD8^+$ T_{RM} cells or to guide $CD8^+$ T_{EM} and T_{CM} cells from the circulation into latently infected TG. Thus, during latency, TGs appear to be more immunologically restrictive and are not "open" to homing $CD8^+$ T_{EM} and T_{CM} cells that would migrate from the circulation into infected TGs (1). In this study, we found that local delivery of the T cell-attracting CXCL10 chemokine, but not of CXCL9 or CCL5 chemokines, dramatically increased both the number and function of HSV-specific $CD8^+$ T_{EM} and T_{RM} cell sub-populations in latently infected TG, improving protection against recurrent ocular herpes infection and disease following UV-B induced reactivation from latently infected TG of HLA-A*0201 Tg mice. The effect of CXCL10 treatment on activation and expansion of $CD8^+$ T cells in TG occurs only in mice that were exposed to UV-B reactivation indicating that local exposure to HSV-1 antigens is crucial. These results suggest that: (*i*) the number and/or the function of $CD8^+$ T cells specific for "ASYMP" epitopes is suppressed in latently infected human TG; (*ii*) local delivery of the T cell-attracting CXCL10 chemokine will expand the repertoire and function of HSV-specific $CD8^+$ T cells and reduce the likelihood of viral reactivation from latency; and (*iii*) a prime/pull vaccine strategy that increases the number and/or function of $CD8^+$ T cells in latently infected TG over a certain threshold would likely lead to protection in humans. The success of this innovative prime/pull therapeutic vaccine is likely due to the expansion and survival characteristics of $CD8^+$ T cell precursors as well as the increase in number and function of other immune cells in TG, including $CD4^+$ T cells and APCs, following CXCL10 treatement. This contributes not only to homing of $CD8^+$ T_{EM} cell sub-populations in latently infected TG, but also to increased expansion and survival of the local tissue-resident $CD8^+$ T_{RM} cells that already exist within the TG.

In this study, we detected high frequencies of HLA-A*0201-restricted $CD8^+$ T cells specific to HSV-1 epitopes. These high frequencies are surprising since the tetramer analyses were performed *ex vivo*, and that the frequencies of T cells binding each tetramer were expected to account for a few percentages of the total cells. If all of the tetramers-specific $CD8^+$ T cells were added together, then large percentages of the entire $CD8^+$ T cell repertoire would be accounted for by HSV-1 epitopes that are binding to HLA-A2 molecules. Given that there are other immunodominant viruses (e.g. EBV), as well as most likely other HLA restrictions, the percentages measured in this study should be interpreted with caution. It is possible that cross-reactivity with other epitopes within or outside the herpes family might also account for the high frequencies of at least some epitopes. Broadly reactive human $CD8^+$ T cells that recognize an epitope conserved between VZV, HSV and EBV have been recently reported by Ahmed *et al.*, 2014 (53). An extensive $CD4^+$ and $CD8^+$ T cell cross-reactivity between alphaherpesviruses has been also recently by Koelle *et al.*, 2016 (27). Cross-reactivity between seemingly unrelated epitopes have also been reported by Welsh, Selin and colleagues (64, 65). Moreover, compared to the frequencies of $CD8^+$ T cells specific to HSV-2 epitopes detected from genital herpes patients (49, 66), we have consistently detected higher frequencies of HLA-A*0201-restricted $CD8^+$ T cells specific to HSV-1 epitopes from ocular herpes patients (6, 15, 30, 32, 54). At least some of these differences could also be due to differences in cohors of ocular and genital herpes patients.

A side-by-side comparaison of the frequencies of $CD8^+$ T cells specific to HSV-1 and HSV-2 epitopes from ocular or genital herpes patients is warranted and will be the subject of a future report.

The AAV8 vector was not directly involved in reduced recurrent infection and disease seen in the AAV8-CXCL10 prime/pull vaccine since no protection was observed in mice that received empty AAV8 vector alone. The AAV8 vector used in our prime/pull vaccine has rapidly moved to the forefront of human therapies in the past few years (67). Several naturally occurring, tissue-specific AAV serotypes have been isolated (67). We chose AAV8 because: (*i*) it is a neurotropic virus with the potential of persistent transgene expression in neurons (68, 69); (*ii*) it can superinfect HSV latently infected neurons (68); (*iii*) it can accommodate up to 4.7 kb of DNA; and (*iv*) it is nonpathogenic. Clinical trials using AAV vectors showed only transient inflammation while demonstrating clinical benefits (67). No side effects have been observed in HSV-1 infected mice during the 30 days of monitoring following treatment with the neuro-invasive AAV8 vector. However, long-term monitoring of the corneas and TG for pathology associated with AAV8 will be necessary to insure the safety of the vectors for eventual use in patients with herpes keratitis.

In conclusion, the present study: (*i*) identifies previously unreported protective “ASYMP” epitopes that are potentially useful if included in a therapeutic herpes simplex vaccine; (*ii*) characterizes the phenotype and the function of the protective $CD8^+$ T cell sub-populations associated with immunologic control of recurrent herpetic disease; and (*iii*) demonstrates that bolstering the number of functional HSV-specific $CD8^+$ T_{EM} and T_{RM} cells in latently infected TG through HSV-1 human epitopes/CXCL10-based prime/pull therapeutic vaccine protected against virus shedding and reduced recurrent herpetic disease. Results from this pre-clinical study should pave the way towards developing a novel clinical T-cell based vaccine immunotherapy against recurrent ocular herpes.

Supplementary Material

Refer to Web version on PubMed Central for supplementary material.

Acknowledgments

This work is supported by Public Health Service Research R01 Grants EY026103, EY019896 and EY024618 from National Eye Institute (NEI) and R21 Grant AI110902 from National Institutes of allergy and Infectious Diseases (NIAID), by The Discovery Center for Eye Research (DCER) and by a Research to Prevent Blindness (RPB) grant.

This work is dedicated to the memory of late Professor Steven L. Wechsler "Steve" (1948–2016), whose numerous pioneering works on herpes latency laid foundation to this line of research.

We thank Dale Long from the NIH Tetramer Facility (Emory University, Atlanta, GA) for providing the Tetramers used in this study, Barbara Bodenhoefer (RN) from UC Irvine’s Institute for Clinical and Translational Science (ICTS) for helping with blood collections from HSV-1 seropositive symptomatic and asymptomatic individuals and Chen, Wen-Pin for helping with the statistics.

References

1. Srivastava R, Khan AA, Garg S, Syed SA, Furness JN, Vahed H, Pham T, Yu HT, Nesburn AB, BenMohamed L. Human Asymptomatic Epitopes Identified from the Herpes Simplex Virus Tegument Protein VP13/14 (UL47) Preferentially Recall Polyfunctional Effector Memory

CD44highCD62LlowCD8+ TEM Cells and Protect "Humanized" HLA-A*02:01 Transgenic Mice Against Ocular Herpes. J Virol. 2016

2. Samandary S, Kridane-Miledi H, Sandoval JS, Choudhury Z, Langa-Vives F, Spencer D, Chentoufi AA, Lemonnier FA, BenMohamed L. Associations of HLA-A, HLA-B and HLA-C alleles frequency with prevalence of herpes simplex virus infections and diseases across global populations: implication for the development of an universal CD8+ T-cell epitope-based vaccine. Hum Immunol. 2014; 75:715–729. [PubMed: 24798939]
3. Looker KJ, Garnett GP, Schmid GP. An estimate of the global prevalence and incidence of herpes simplex virus type 2 infection. Bull World Health Organ. 2008; 86:805–812. A. [PubMed: 18949218]
4. Zhang X, Dervillez X, Chentoufi AA, Badakhshan T, Bettahi I, Benmohamed L. Targeting the genital tract mucosa with a lipopeptide/recombinant adenovirus prime/boost vaccine induces potent and long-lasting CD8+ T cell immunity against herpes: importance of MyD88. J Immunol. 2012; 189:4496–4509. [PubMed: 23018456]
5. Chentoufi AA, BenMohamed L. Future viral vectors for the delivery of asymptomatic herpes epitope-based immunotherapeutic vaccines. Future virology. 2010; 5:525–528. [PubMed: 21442030]
6. Chentoufi AA, Zhang X, Lamberth K, Dasgupta G, Bettahi I, Nguyen A, Wu M, Zhu X, Mohebbi A, Buus S, Wechsler SL, Nesburn AB, BenMohamed L. HLA-A*0201-restricted CD8+ cytotoxic T lymphocyte epitopes identified from herpes simplex virus glycoprotein D. J Immunol. 2008; 180:426–437. [PubMed: 18097044]
7. Corey L, Langenberg AG, Ashley R, Sekulovich RE, Izu AE, Douglas JM Jr, Handsfield HH, Warren T, Marr L, Tyring S, DiCarlo R, Adimora AA, Leone P, Dekker CL, Burke RL, Leong WP, Straus SE. Recombinant glycoprotein vaccine for the prevention of genital HSV-2 infection: two randomized controlled trials. Chiron HSV Vaccine Study Group. Jama. 1999; 282:331–340. [PubMed: 10432030]
8. Langenberg AG, Corey L, Ashley RL, Leong WP, Straus SE. A prospective study of new infections with herpes simplex virus type 1 and type 2. Chiron HSV Vaccine Study Group. The New England journal of medicine. 1999; 341:1432–1438. [PubMed: 10547406]
9. Chentoufi AA, Dervillez X, Dasgupta G, Nguyen C, Kabbara KW, Jiang X, Nesburn AB, Wechsler SL, BenMohamed L. The herpes simplex virus type 1 latency-associated transcript inhibits phenotypic and functional maturation of dendritic cells. Viral Immunol. 2012; 25:204–215. [PubMed: 22512280]
10. Khan AA, Srivastava R, Chentoufi AA, Geertsema R, Thai NT, Dasgupta G, Osorio N, Kalantari M, Nesburn AB, Wechsler SL, BenMohamed L. Therapeutic immunization with a mixture of herpes simplex virus 1 glycoprotein D-derived "asymptomatic" human CD8+ T-cell epitopes decreases spontaneous ocular shedding in latently infected HLA transgenic rabbits: association with low frequency of local PD-1+ TIM-3+ CD8+ exhausted T cells. J Virol. 2015; 89:6619–6632. [PubMed: 25878105]
11. Dervillez X, Gottimukkala C, Kabbara KW, Nguyen C, Badakhshan T, Kim SM, Nesburn AB, Wechsler SL, Benmohamed L. Future of an "Asymptomatic" T-cell Epitope-Based Therapeutic Herpes Simplex Vaccine. Future virology. 2012; 7:371–378. [PubMed: 22701511]
12. Kuo T, Wang C, Badakhshan T, Chilukuri S, BenMohamed L. The challenges and opportunities for the development of a T-cell epitope-based herpes simplex vaccine. Vaccine. 2014; 32:6733–6745. [PubMed: 25446827]
13. BenMohamed L, Osorio N, Srivastava R, Khan AA, Simpson JL, Wechsler SL. Decreased reactivation of a herpes simplex virus type 1 (HSV-1) latency-associated transcript (LAT) mutant using the in vivo mouse UV-B model of induced reactivation. J Neurovirol. 2015
14. BenMohamed L, Osorio N, Khan AA, Srivastava R, Huang L, Krochma JJ, Garcia LM, Simpson JL, Wechsler SL. Prior Corneal Scarification and Injection of Immune Serum are not Required Before Ocular HSV-1 Infection for UV-B Induced Virus Reactivation and Recurrent Herpetic Corneal Disease in Latently Infected Mice. Journal of neurovirology. 2015
15. Srivastava R, Khan AA, Spencer D, Vahed H, Lopes PP, Thai NT, Wang C, Pham TT, Huang J, Scarfone VM, Nesburn AB, Wechsler SL, BenMohamed L. HLA-A02:01-restricted epitopes identified from the herpes simplex virus tegument protein VP11/12 preferentially recall

polyfunctional effector memory CD8+ T cells from seropositive asymptomatic individuals and protect humanized HLA-A*02:01 transgenic mice against ocular herpes. J Immunol. 2015; 194:2232–2248. [PubMed: 25617474]

16. Chentoufi AA, Dasgupta G, Nesburn AB, Bettahi I, Binder NR, Choudhury ZS, Chamberlain WD, Wechsler SL, BenMohamed L. Nasolacrimal duct closure modulates ocular mucosal and systemic CD4(+) T-cell responses induced following topical ocular or intranasal immunization. Clinical and vaccine immunology : CVI. 2010; 17:342–353. [PubMed: 20089796]
17. Dasgupta G, Nesburn AB, Wechsler SL, BenMohamed L. Developing an asymptomatic mucosal herpes vaccine: the present and the future. Future Microbiol. 2010; 5:1–4. [PubMed: 20020824]
18. Chentoufi AA, Dasgupta G, Christensen ND, Hu J, Choudhury ZS, Azeem A, Jester JV, Nesburn AB, Wechsler SL, BenMohamed L. A Novel Human Leukocyte Antigen (HLA-A*0201) Transgenic Rabbit Model for Pre-clinical Evaluation of Human CD8+ T-Cell Epitope-Based Vaccines Against Ocular Herpes. J Immunol. 2009 In press: 00-00.
19. Dasgupta G, Chentoufi AA, Nesburn AB, Wechsler SL, BenMohamed L. New concepts in herpes simplex virus vaccine development: notes from the battlefield. Expert Rev Vaccines. 2009; 8:1023–1035. [PubMed: 19627185]
20. Zhang X, Chentoufi AA, Dasgupta G, Nesburn AB, Wu M, Zhu X, Carpenter D, Wechsler SL, You S, BenMohamed L. A genital tract peptide epitope vaccine targeting TLR-2 efficiently induces local and systemic CD8+ T cells and protects against herpes simplex virus type 2 challenge. Mucosal Immunol. 2009; 2:129–143. [PubMed: 19129756]
21. Stanberry LR. Clinical trials of prophylactic and therapeutic herpes simplex virus vaccines. Herpes. 2004; 11(Suppl 3):161A–169A.
22. Belshe PB, Leone PA, Bernstein DI, Wald A, Levin MJ, Stapleton JT, Gorfinkel I, Morrow RLA, Ewell MG, Stokes-Riner A, Dubin G, Heineman TC, Schulte JM, Deal CD. Efficacy Results of a Trial of a Herpes Simplex Vaccine. The New England journal of medicine. 2012; 366:34–43. [PubMed: 22216840]
23. Chentoufi AA, Dasgupta G, Christensen ND, Hu J, Choudhury ZS, Azeem A, Jester JV, Nesburn AB, Wechsler SL, BenMohamed L. A novel HLA (HLA-A*0201) transgenic rabbit model for preclinical evaluation of human CD8+ T cell epitope-based vaccines against ocular herpes. J Immunol. 2010; 184:2561–2571. [PubMed: 20124097]
24. Dasgupta G, BenMohamed L. Of mice and not humans: how reliable are animal models for evaluation of herpes CD8(+)-T cell-epitopes-based immunotherapeutic vaccine candidates? Vaccine. 2011; 29:5824–5836. [PubMed: 21718746]
25. Koelle DM, Gonzalez JC, Johnson AS. Homing in on the cellular immune response to HSV-2 in humans. Am J Reprod Immunol. 2005; 53:172–181. [PubMed: 15760378]
26. Posavad CM, Huang ML, Barcy S, Koelle DM, Corey L. Long term persistence of herpes simplex virus-specific CD8+ CTL in persons with frequently recurring genital herpes. J Immunol. 2000; 165:1146–1152. [PubMed: 10878394]
27. Jing L, Laing KJ, Dong L, Russell RM, Barlow RS, Haas JG, Ramchandani MS, Johnston C, Buus S, Redwood AJ, White KD, Mallal SA, Phillips EJ, Posavad CM, Wald A, Koelle DM. Extensive CD4 and CD8 T Cell Cross-Reactivity between Alphaherpesviruses. J Immunol. 2016; 196:2205–2218. [PubMed: 26810224]
28. Chentoufi AA, Kritzer E, Yu DM, Nesburn AB, Benmohamed L. Towards a rational design of an asymptomatic clinical herpes vaccine: the old, the new, and the unknown. Clin Dev Immunol. 2012; 2012:187585. [PubMed: 22548113]
29. Dasgupta G, Chentoufi AA, Kalantari M, Falatoonzadeh P, Chun S, Lim CH, Felgner PL, Davies DH, BenMohamed L. Immunodominant "asymptomatic" herpes simplex virus 1 and 2 protein antigens identified by probing whole-ORFome microarrays with serum antibodies from seropositive asymptomatic versus symptomatic individuals. J Virol. 2012; 86:4358–4369. [PubMed: 22318137]
30. Dervillez X, Qureshi H, Chentoufi AA, Khan AA, Kritzer E, Yu DC, Diaz OR, Gottimukkala C, Kalantari M, Villacres MC, Scarfone VM, McKinney DM, Sidney J, Sette A, Nesburn AB, Wechsler SL, BenMohamed L. Asymptomatic HLA-A*02:01-restricted epitopes from herpes simplex virus glycoprotein B preferentially recall polyfunctional CD8+ T cells from seropositive

asymptomatic individuals and protect HLA transgenic mice against ocular herpes. J Immunol. 2013; 191:5124–5138. [PubMed: 24101547]

31. Khan AA, Srivastava R, Lopes PP, Wang C, Pham TT, Cochrane J, Thai NT, Gutierrez L, Benmohamed L. Asymptomatic memory CD8+ T cells: from development and regulation to consideration for human vaccines and immunotherapeutics. Hum Vaccin Immunother. 2014; 10:945–963. [PubMed: 24499824]
32. Khan AA, Srivastava R, Spencer D, Garg S, Fremgen D, Vahed H, Lopes PP, Pham TT, Hewett C, Kuang J, Ong N, Huang L, Scarfone VM, Nesburn AB, Wechsler SL, BenMohamed L. Phenotypic and functional characterization of herpes simplex virus glycoprotein B epitope-specific effector and memory CD8+ T cells from symptomatic and asymptomatic individuals with ocular herpes. J Virol. 2015; 89:3776–3792. [PubMed: 25609800]
33. Srivastava R, Khan AA, J H, Nesburn AB, Wechsler SL, BenMohamed L. Herpes Simplex Virus Type 1 Human Asymptomatic CD8 T cell Epitopes Protect Against Ocular Herpes in "Humanized" HLA Transgenic Rabbit Model. IOVS. 2015; 194:2232–2248.
34. Banerjee K, Biswas PS, Rouse BT. Elucidating the protective and pathologic T cell species in the virus-induced corneal immunoinflammatory condition herpetic stromal keratitis. J Leukoc Biol. 2005; 77:24–32. [PubMed: 15496448]
35. Himmelein S, St Leger AJ, Knickelbein JE, Rowe A, Freeman ML, Hendricks RL. Circulating herpes simplex type 1 (HSV-1)-specific CD8+ T cells do not access HSV-1 latently infected trigeminal ganglia. Herpesviridae. 2011; 2:5. [PubMed: 21429183]
36. Sidney J, Southwood S, Moore C, Oseroff C, Pinilla C, Grey HM, Sette A. Measurement of MHC/peptide interactions by gel filtration or monoclonal antibody capture. Curr Protoc Immunol. 2013 Chapter 18: Unit 18 13.
37. Chentoufi AA, Binder NR, Berka N, Durand G, Nguyen A, Bettahi I, Maillere B, BenMohamed L. Asymptomatic human CD4+ cytotoxic T-cell epitopes identified from herpes simplex virus glycoprotein B. J Virol. 2008; 82:11792–11802. [PubMed: 18799581]
38. Nesburn AB, Bettahi I, Zhang X, Zhu X, Chamberlain W, Afifi RE, Wechsler SL, BenMohamed L. Topical/mucosal delivery of sub-unit vaccines that stimulate the ocular mucosal immune system. Ocul Surf. 2006; 4:178–187. [PubMed: 17146573]
39. Cheng Y, Prusoff WH. Relationship between the inhibition constant (K1) and the concentration of inhibitor which causes 50 per cent inhibition (I50) of an enzymatic reaction. Biochem Pharmacol. 1973; 22:3099–3108. [PubMed: 4202581]
40. Mashiba T, Udaka K, Hirachi Y, Hiasa Y, Miyakawa T, Satta Y, Osoda T, Kataoka S, Kohara M, Onji M. Identification of CTL epitopes in hepatitis C virus by a genome-wide computational scanning and a rational design of peptide vaccine. Immunogenetics. 2007; 59:197–209. [PubMed: 17225159]
41. Geluk A, van Meijgaarden KE, Joosten SA, Commandeur S, Ottenhoff TH. Innovative Strategies to Identify M. tuberculosis Antigens and Epitopes Using Genome-Wide Analyses. Front Immunol. 2014; 5:256. [PubMed: 25009541]
42. Nesburn AB, Burke RL, Ghiasi H, Slanina SM, Wechsler SL. A therapeutic vaccine that reduces recurrent herpes simplex virus type 1 corneal disease. Invest Ophthalmol Vis Sci. 1998; 39:1163–1170. [PubMed: 9620075]
43. Mott KR, Chentoufi AA, Carpenter D, BenMohamed L, Wechsler SL, Ghiasi H. The role of a glycoprotein K (gK) CD8+ T-cell epitope of herpes simplex virus on virus replication and pathogenicity. Invest Ophthalmol Vis Sci. 2009; 50:2903–2912. [PubMed: 19168902]
44. Zhang X, Issagholian A, Berg EA, Fishman JB, Nesburn AB, BenMohamed L. Th-cytotoxic T-lymphocyte chimeric epitopes extended by Nepsilon-palmitoyl lysines induce herpes simplex virus type 1-specific effector CD8+ Tc1 responses and protect against ocular infection. J Virol. 2005; 79:15289–15301. [PubMed: 16306600]
45. Zhu X, Ramos TV, Gras-Masse H, Kaplan BE, BenMohamed L. Lipopeptide epitopes extended by an Nepsilon-palmitoyl-lysine moiety increase uptake and maturation of dendritic cells through a Toll-like receptor-2 pathway and trigger a Th1-dependent protective immunity. Eur J Immunol. 2004; 34:3102–3114. [PubMed: 15368273]

46. St Leger AJ, Hendricks RL. CD8(+) T cells patrol HSV-1-infected trigeminal ganglia and prevent viral reactivation. J Neurovirol. 2011
47. St Leger AJ, Peters B, Sidney J, Sette A, Hendricks RL. Defining the herpes simplex virus-specific CD8+ T cell repertoire in C57BL/6 mice. J Immunol. 2011; 186:3927–3933. [PubMed: 21357536]
48. van Velzen M, Jing L, Osterhaus AD, Sette A, Koelle DM, Verjans GM. Local CD4 and CD8 T-cell reactivity to HSV-1 antigens documents broad viral protein expression and immune competence in latently infected human trigeminal ganglia. PLoS Pathog. 2013; 9:e1003547. [PubMed: 23966859]
49. Jing L, Haas J, Chong TM, Bruckner JJ, Dann GC, Dong L, Marshak JO, McClurkan CL, Yamamoto TN, Bailer SM, Laing KJ, Wald A, Verjans GM, Koelle DM. Cross-presentation and genome-wide screening reveal candidate T cells antigens for a herpes simplex virus type 1 vaccine. J Clin Invest. 2012; 122:654–673. [PubMed: 22214845]
50. Hosken N, McGowan P, Meier A, Koelle DM, Sleath P, Wagener F, Elliott M, Grabstein K, Posavad C, Corey L. Diversity of the CD8+ T-cell response to herpes simplex virus type 2 proteins among persons with genital herpes. J Virol. 2006; 80:5509–5515. [PubMed: 16699031]
51. Koelle DM, Abbo H, Peck A, Ziegweid K, Corey L. Direct recovery of herpes simplex virus (HSV)-specific T lymphocyte clones from recurrent genital HSV-2 lesions. The Journal of infectious diseases. 1994; 169:956–961. [PubMed: 8169426]
52. St Leger AJ, Jeon S, Hendricks RL. Broadening the Repertoire of Functional Herpes Simplex Virus Type 1-Specific CD8+ T Cells Reduces Viral Reactivation from Latency in Sensory Ganglia. J Immunol. 2013; 191:2258–2265. [PubMed: 23878317]
53. Chiu C, McCausland M, Sidney J, Duh FM, Rouphael N, Mehta A, Mulligan M, Carrington M, Wieland A, Sullivan NL, Weinberg A, Levin MJ, Pulendran B, Peters B, Sette A, Ahmed R. Broadly reactive human CD8 T cells that recognize an epitope conserved between VZV, HSV and EBV. PLoS Pathog. 2014; 10:e1004008. [PubMed: 24675761]
54. Srivastava R, Khan AA, Garg S, Syed SA, Furness JN, Vahed H, Pham T, Yu HT, Nesburn AB, BenMohamed L. Human Asymptomatic Epitopes Identified from the Herpes Simplex Virus Tegument Protein VP13/14 (UL47) Preferentially Recall Polyfunctional Effector Memory CD44high CD62Llow CD8+ TEM Cells and Protect Humanized HLA-A*02:01 Transgenic Mice against Ocular Herpesvirus Infection. J Virol. 2017; 91
55. Feldman LT, Ellison AR, Voytek CC, Yang L, Krause P, Margolis TP. Spontaneous molecular reactivation of herpes simplex virus type 1 latency in mice. Proc Natl Acad Sci U S A. 2002; 99:978–983. [PubMed: 11773630]
56. Nesburn AB, Burke RL, Ghiasi H, Slanina SM, Wechsler SL. Therapeutic periocular vaccination with a subunit vaccine induces higher levels of herpes simplex virus-specific tear secretory immunoglobulin A than systemic vaccination and provides protection against recurrent spontaneous ocular shedding of virus in latently infected rabbits. Virology. 1998; 252:200–209. [PubMed: 9875329]
57. Lepisto AJ, Frank GM, Xu M, Stuart PM, Hendricks RL. CD8 T cells mediate transient herpes stromal keratitis in CD4-deficient mice. Invest Ophthalmol Vis Sci. 2006; 47:3400–3409. [PubMed: 16877409]
58. Hendricks RL. Immunopathogenesis of viral ocular infections. Chem Immunol. 1999; 73:120–136. [PubMed: 10590577]
59. Stuart PM, Keadle TL. Recurrent herpetic stromal keratitis in mice: a model for studying human HSK. Clin Dev Immunol. 2012; 88:72–78.
60. Morris J, Stuart PM, Rogge M, Potter C, Gupta N, Yin XT. Recurrent herpetic stromal keratitis in mice, a model for studying human HSK. J Vis Exp. 2012; 88:33–39.
61. Webre JM, Hill JM, Nolan NM, Clement C, McFerrin HE, Bhattacharjee PS, Hsia V, Neumann DM, Foster TP, Lukiw WJ, Thompson HW. Rabbit and mouse models of HSV-1 latency, reactivation, and recurrent eye diseases. J Biomed Biotechnol. 2012; 7:12–16.
62. Dervillez X, Qureshi H, Chentoufi AA, Khan AA, Kritzer K, Yu DC, Diaz OR, Gottimukkala C, Kalantari M, Villacres MC, Scarfone VM, McKinney DM, Sidney J, Sette A, Nesburn AB, Wechsler SL, BenMohamed L. “Asymptomatic” HLA-A*02:01-Restricted Epitopes from Herpes Simplex Virus Glycoprotein B Preferentially Recall Polyfunctional CD8+ T Cells from

Seropositive Asymptomatic Individuals and Protect HLA Transgenic Mice Against Ocular Herpes. J Immunol. 2013

63. Held K, Junker A, Dornmair K, Meinl E, Sinicina I, Brandt T, Theil D, Derfuss T. Expression of herpes simplex virus 1-encoded microRNAs in human trigeminal ganglia and their relation to local T-cell infiltrates. J Virol. 2011; 85:9680–9685. [PubMed: 21795359]
64. Cornberg M, Clute SC, Watkin LB, Saccoccio FM, Kim SK, Naumov YN, Brehm MA, Aslan N, Welsh RM, Selin LK. CD8 T cell cross-reactivity networks mediate heterologous immunity in human EBV and murine vaccinia virus infections. Journal of immunology. 2010; 184:2825–2838.
65. Welsh RM, Che JW, Brehm MA, Selin LK. Heterologous immunity between viruses. Immunol Rev. 2010; 235:244–266. [PubMed: 20536568]
66. Laing KJ, Magaret AS, Mueller DE, Zhao L, Johnston C, De Rosa SC, Koelle DM, Wald A, Corey L. Diversity in CD8(+) T cell function and epitope breadth among persons with genital herpes. J Clin Immunol. 2010; 30:703–722. [PubMed: 20635156]
67. Wu Z, Asokan A, Samulski RJ. Adeno-associated virus serotypes: vector toolkit for human gene therapy. Mol Ther. 2006; 14:316–327. [PubMed: 16824801]
68. Liu J, Lewin AS, Tuli SS, Ghivizzani SC, Schultz GS, Bloom DC. Reduction in severity of a herpes simplex virus type 1 murine infection by treatment with a ribozyme targeting the UL20 gene RNA. J Virol. 2008; 82:7467–7474. [PubMed: 18508896]
69. Foust KD, Poirier A, Pacak CA, Mandel RJ, Flotte TR. Neonatal intraperitoneal or intravenous injections of recombinant adeno-associated virus type 8 transduce dorsal root ganglia and lower motor neurons. Hum Gene Ther. 2008; 19:61–70. [PubMed: 18052722]

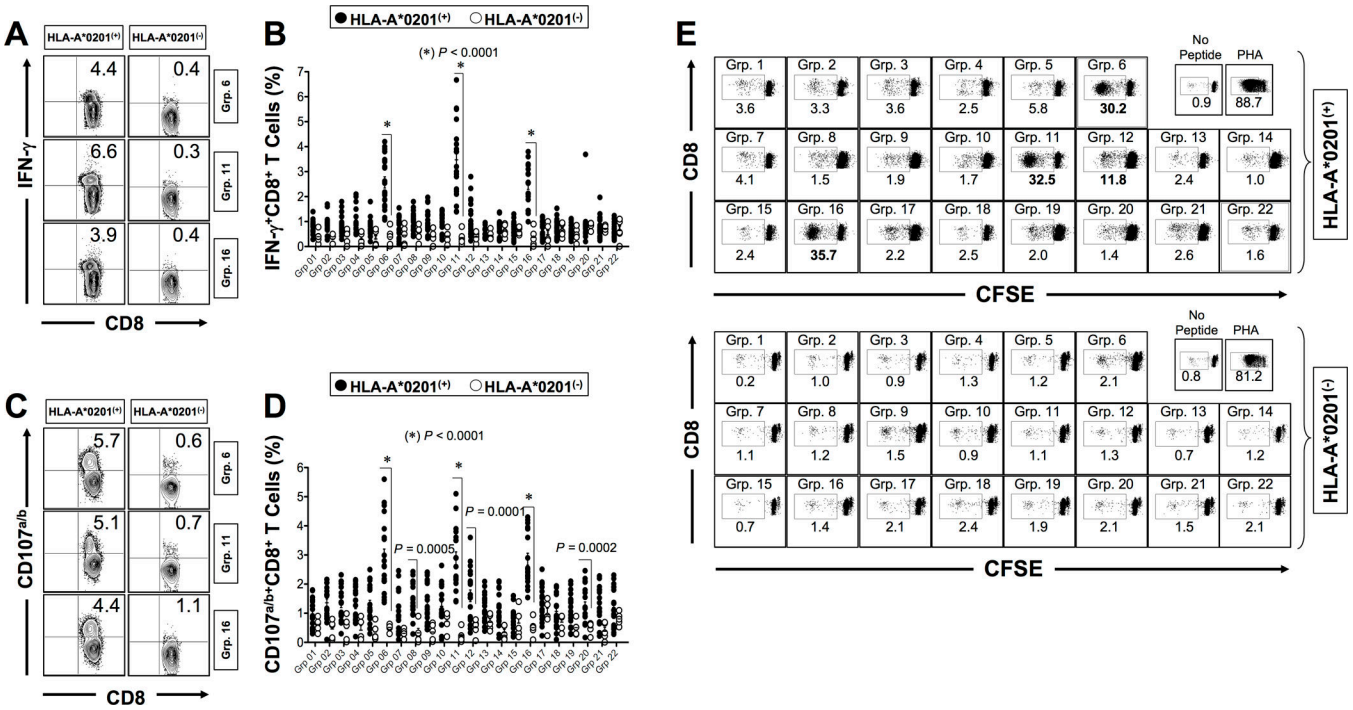

Figure 1. Frequency of IFN-γ-producing CD8$^+$ T cells specific to genome wide-derived epitopes in HLA-A*0201$^{(+)}$ HSV-seropositive individuals

PBMCs (~10 × 10^6) derived from 20 HLA-A*0201$^{(+)}$ individuals vs. 8 HLA-A*0201$^{(-)}$ HSV-seropositive individuals were stimulated *in vitro* for 72 hrs with each of 22 groups of equimolar peptides. IFN-γ and CD107$^{a/b}$ were then measured by intracellular staining, as outlined in *Materials and Methods*. (**A**) Representative contour plots of percentage of IFN-γ$^+$CD8$^+$ T cells specific to groups of HSV-1 peptides 6, 11 and 16 detected in HLA-A*0201$^{(+)}$ (left panels) and HLA-A*0201$^{(-)}$ (right panels) individuals. (**B**) Average frequencies of IFN-γ$^+$CD8$^+$ T cells specific to 22 groups of HSV-1 peptides detected in PBMCs from HLA-A*0201$^{(+)}$ (closed circle) and HLA-A*0201$^{(-)}$ (open circle) individuals. (**C**) Representative contour plots of expression of CD107$^{a/b}$ by CD8$^+$ T cells specific to groups of HSV-1 peptides 6, 11 and 16 detected in HLA-A*0201$^{(+)}$ (left panel) and HLA-A*0201$^{(-)}$ (right panel) individuals. (**D**) Average frequencies of CD107$^{a/b(+)}$CD8$^+$ T cells detected in HLA-A*0201$^{(+)}$ (closed circle) and HLA-A*0201$^{(-)}$ (open circle) individuals in response to 22 groups of HSV-1 peptides. (**E**) Representative dot plots of percentage of dividing CFSE$^{(+)}$CD8$^+$ T cells from HLA-A*0201$^{(+)}$ (top three rows) and HLA-A*0201$^{(-)}$ individuals (lower three rows) following a 6-days *in vitro* stimulation with each of the 22 groups of HSV-1 peptides. The results are representative of 2 independent experiments. The nominal *P* values indicated on panels (**B**) and (**D**) show statistical significance between HLA-A*0201$^{(+)}$ and HLA-A*0201$^{(-)}$ individuals. *P* values are calculated using either the parametric two-sample Student's *t*-test or non-parametric Wilcoxon rank sum test, as appropriate. For paired comparisons involving the 22 groups of peptides, we have adjusted for multiple comparisons using the Bonferroni procedure.

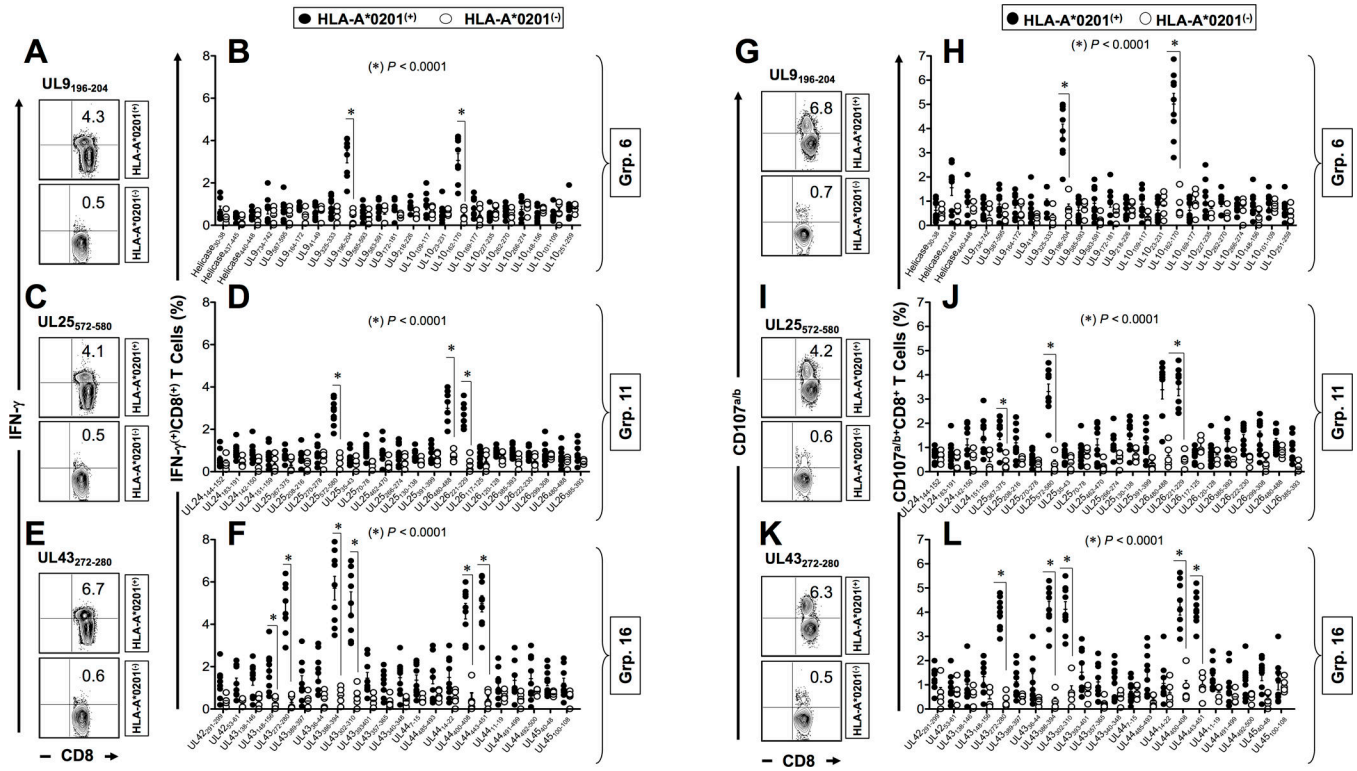

Figure 2. IFN-γ-producing CD8$^+$ T cell responses to HSV-1 individual epitopes detected from HLA-A*0201$^{(+)}$ HSV-seropositive individuals

PBMCs (~10 × 10^6) derived from 10 HLA-A*0201$^{(+)}$ individuals vs. 8 HLA-A*0201$^{(−)}$ HSV-seropositive individuals were stimulated *in vitro* for 72-hours with individual CD8$^+$ T cell epitope peptides (a total of 68 peptides, at 10μg/ml each) derived from Grp. 6, Grp. 11 and Grp. 16 of HSV-1 peptides (see Fig. 1). Representative FACS contour plots showing percentage of IFN-γ$^+$CD8$^+$ T cells detected from one HLA-A*0201$^{(+)}$ individual (top plot) and HLA-A*0201$^{(−)}$ individual (bottom plot) following stimulation with UL9$_{196–204}$ (**A**), UL25$_{572–580}$ (**C**) and UL43$_{272–280}$ (**E**) immunodominant peptides respectively from groups of HSV-1 peptide Grp. 6, Grp. 11 and Grp. 16. Average frequencies of IFN-γ$^+$CD8$^+$ T cells detected in 10 HLA-A*0201$^{(+)}$ individuals (closed circle) vs. 8 HLA-A*0201$^{(−)}$ individuals (open circles) in response to *in vitro* stimulation with individual peptides from Grp. 6 (**B**), Grp. 11 (**D**) and Grp. 16 (**F**) of HSV-1 peptides. Representative FACS contour plots showing percentage of CD107$^{a/b(+)}$CD8$^+$ T cells detected from one HLA-A*0201$^{(+)}$ individual (top plot) and HLA-A*0201$^{(−)}$ individual (bottom plot) following stimulation with UL9$_{196–204}$ (**G**), UL25$_{572–580}$ (**I**) and UL43$_{272–280}$ (**K**) immunodominant peptides from Grp. 6, Grp. 11 and Grp. 16 of HSV-1 peptides, respectively. Average frequencies of CD107$^{a/b(+)}$CD8$^+$ T cells detected in 10 HLA-A*0201$^{(+)}$ individuals (closed circle) vs. 8 HLA-A*0201$^{(−)}$ individuals (open circles) in response to *in vitro* stimulation with individual peptides from Grp. 6 (**H**), Grp. 11 (**J**) and Grp. 16 (**L**) of HSV-1 peptides. The results are representative of 2 independent experiments. The nominal *P* values indicated on panels (**B**), (**D**), (**F**), (**H**), (**J**) and (**L**) show statistical significance between HLA-A*0201$^{(+)}$ and HLA-A*0201$^{(−)}$ individuals. *P* values are calculated using either the parametric two-sample Student's *t*-test or non-parametric Wilcoxon rank sum test, as appropriate. For paired comparisons involving

individual peptides we have adjusted for multiple comparisons using the Bonferroni procedure.

A

Potential HLA-A*0201 restricted epitopes selected from herpes simplex virus genome wide proteins

Peptide	Sequence	MW	BIMAS[a]	SYFPEITHI[b]	MHCPred[c]	A*0201 binding capacity (IC_{50} nM)		Protein	T2 Assay (% MFI)			Gene
						Predicted	Measured		12μM	6μM	3μM	
$UL9_{(196-204)}$	ALMLRLLRI	1098.40	88.78	26	0.40	35	46	Replication Origin Binding Protein UL9	398.0	355.0	307.8	Beta
$UL10_{(162-170)}$	SQLAHLVYV	1029.20	330.06	20	0.27	9.4	62	Envelope Glycoprotein M UL10	301.6	284.0	271.0	Gamma 2
$UL25_{(572-580)}$	FIPQYLSAV	1037.23	101.18	25	0.06	17	15	DNA Packaging Tegument Protein UL25	291.2	293.4	247.7	Gamma 2
$UL26_{(480-488)}$	ALMGAVTSL	862.06	181.79	31	0.59	11	4.2	Capsid Maturation Protease UL26	374.2	274.9	236.8	Gamma
$UL26_{(221-229)}$	MMLRDRWSL	1207.49	727.84	22	0.49	15	14	Capsid Maturation Protease UL26	277.0	267.6	222.4	Gamma
$UL43_{(272-280)}$	FLGAGALAV	817.98	319.94	25	-0.12	16	80	Envelope Protein UL43	392.6	295.4	286.7	Gamma
$UL43_{(386-394)}$	TLRGLFFSV	1039.25	58.25	25	0.17	46	94	Envelope Protein UL43	358.5	301.8	255.1	Gamma
$UL43_{(302-310)}$	FLGGHVAVA	870.01	21.55	23	-0.48	34	65	Envelope Protein UL43	377.0	261.4	232.6	Gamma
$UL44_{(400-408)}$	FLGDDPSPA	917.98	93.70	16	-0.48	19	13	Envelope Glycoprotein C UL44	254.1	223.8	212.8	Gamma 2
$UL44_{(443-451)}$	RLTGYPAGI	947.11	10.43	23	0.30	47	1099	Envelope Glycoprotein C UL44	241.1	227.6	205.9	Gamma 2

Genome wide sequence of HSV-1 84+ proteins were submitted to screening of potential HLA-A*0201 epitopes using several computer algorithms. Ten peptides were selected based on functional assays and stabilization of HLA-A*0201 molecules on the surface of T2 cells. Predicted IC_{50} values as calculated by BIMAS[(a)]: http://www-bimas.cit.nih.gov/molbio/hla_bind; SYFPEITHI[(b)]: http://www.syfpeithi.de; and MHCPred[(c)]:http://www.mhc-pathway.net. The sequences of synthesized peptides are based on the HSV-1 strain 17

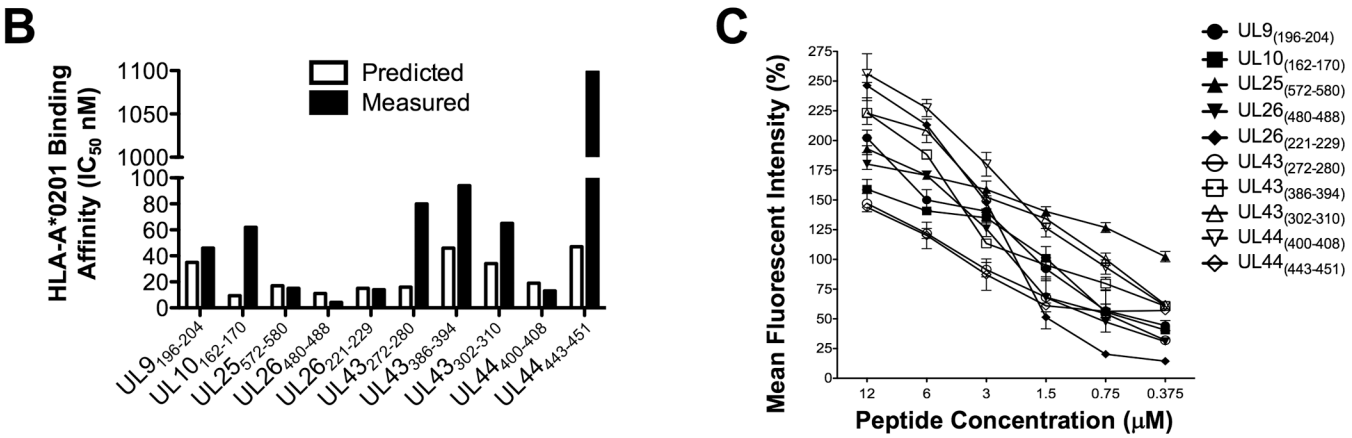

Figure 3. Potential epitope peptides bind with high affinity to HLA-A*0201 and stabilizes its expression on the surface of target cells

(**A**) Ten potential epitopes with high predicted affinity to the HLA-A*0201 molecule identified from the amino acid genome sequence of HSV1 (strain 17) using BIMAS, SYFPEITHI and MAPPP computational algorithms. (**B**) Predicted and measured binding affinity of genome-derived peptide epitopes to soluble HLA-A*0201 molecule (IC_{50} nM). (**C**) Stabilization of HLA-A*0201 molecules on the surface of T_2 cells by VP13/14 peptide epitopes. T_2 cells (3×10^5) were incubated with serial dilutions of the indicated genome-derived peptides, as described in *Materials & Methods*. Cells were then stained with FITC conjugated anti-HLA-A2 mAb (BB7.2). The graph represents the increase in the expression of HLA-A2 molecules on the surface of T_2 cells triggered by various concentrations of genome-derived peptides and represented as percent of mean fluorescence intensity (MFI): Percent of MFI increase = (MFI with the given peptide − MFI without peptide) / (MFI without peptide) × 100. Error bars show standard deviation (SD) obtained from 3 independent experiments.

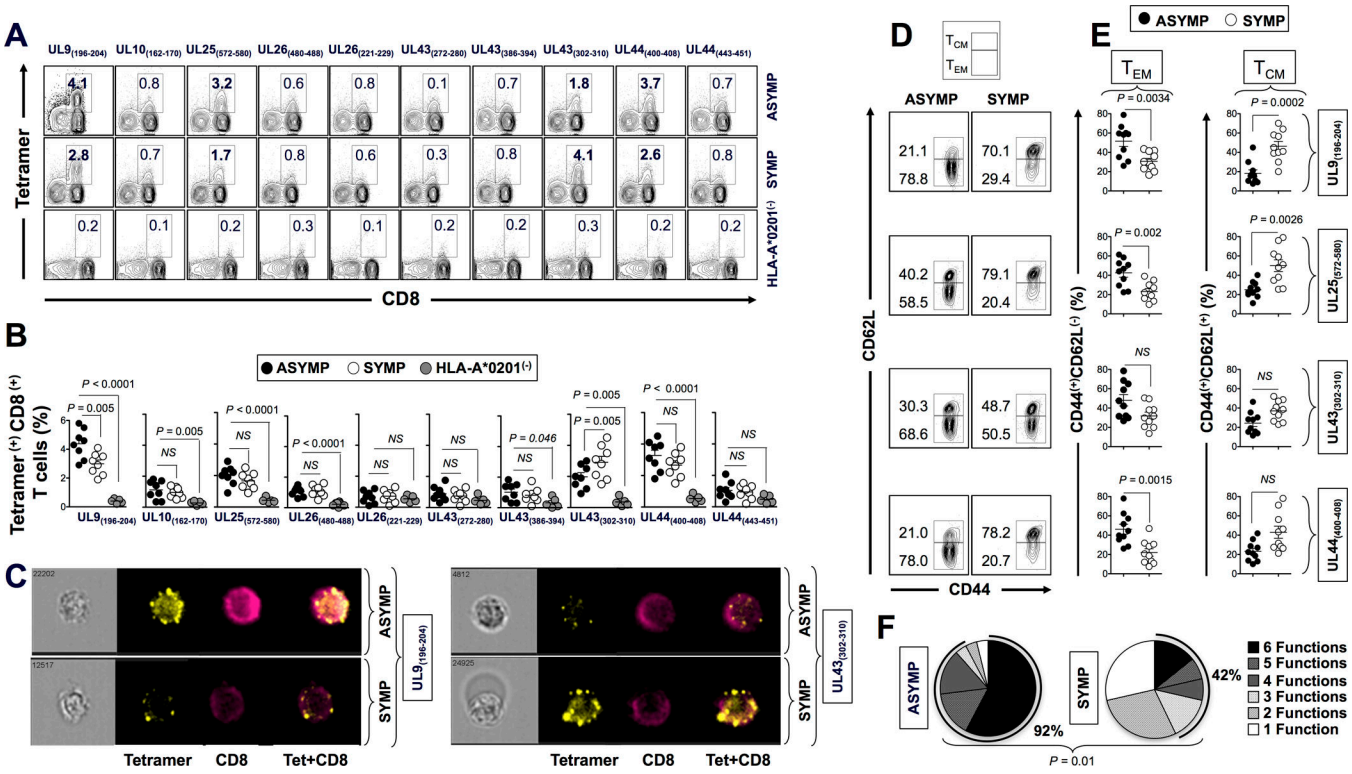

Figure 4. Frequencies of HSV-1 epitopes-specific CD8$^+$ T_{CM} and T_{EM} cells detected in HSV-seropositive SYMP and ASYMP individuals

(**A**) The representative FACS plots of tetramer specific CD8$^+$ T cells. Top row shows contour plots of individual tetramer specific CD8$^+$ T cells detected in one HLA-A*0201$^{(+)}$ HSV-1-seropositive ASYMP individual. Middle row shows contour plots of individual tetramer specific CD8$^+$ T cells detected in one HLA-A*0201$^{(+)}$ HSV-1-seropositive SYMP individual. Bottom row shows contour plots of individual tetramer specific CD8$^+$ T cells detected in one HLA-A*0201$^{(−)}$ control individual. (**B**) Average frequencies of CD8$^+$ T cells specific to ten immunodominant HSV-1 genome-derived epitopes detected in 10 HLA-A*0201$^{(+)}$ ASYMP (closed circle), 8 HLA-A*0201$^{(+)}$ SYMP (open circle) and HLA-A*0201$^{(−)}$ controls (grey filled circles). The nominal *P* values indicated on panel (**B**) show statistical significance between SYMP/ASYMP vs. HLA-A*0201$^{(−)}$ individuals. We have used the General Linear Model procedure and compared the least squares means using the Dunnett procedure for multiple comparisons. (**C**) ImageStram of individual CD8$^+$ T cells derived from one ASYMP vs. SYMP individual, stained with a tetramer specific to the "ASYMP" UL9$_{196–204}$ epitope (*left two panels*) or with a tetramer specific to the "SYMP" UL43$_{302–310}$ epitope (*right two panels*). (**D**) Representative FACS plot of CD44^{high}CD62^{high}CD8$^+$ T_{CM} cells and CD44^{high}CD62^{low}CD8$^+$ T_{EM} cells specific to UL9$_{196–204}$ epitope detected from one ASYMP individual (l*eft contour plots*) vs. one SYMP individual (*right contour plots*). (**E**) Average frequency of T_{CM} and T_{EM} cell specific to UL9$_{196–204}$, UL25$_{572–580}$, UL43$_{302–310}$ and UL44$_{400–408}$ epitopes detected from 10 ASYMP (*closed circles*) and 8 SYMP individuals (*open circles*). The nominal *P* values indicated on panel (**E**) show statistical significance between SYMP and ASYMP individuals. *P* values are calculated using either the parametric two-sample Student's *t*-test

or non-parametric Wilcoxon rank sum test. For paired comparisons involving individual peptides we have adjusted for multiple comparisons using the Bonferroni procedure. (**F**) Pie charts representing the overall mean number of cumulative $CD8^+$ T cell functions in response to stimulation with individual peptides detected in HLA-A*0201$^{(+)}$ ASYMP individuals (*left*) vs. HLA-A*0201$^{(+)}$ SYMP individuals (*right*). The results are representative of 2 independent experiments.

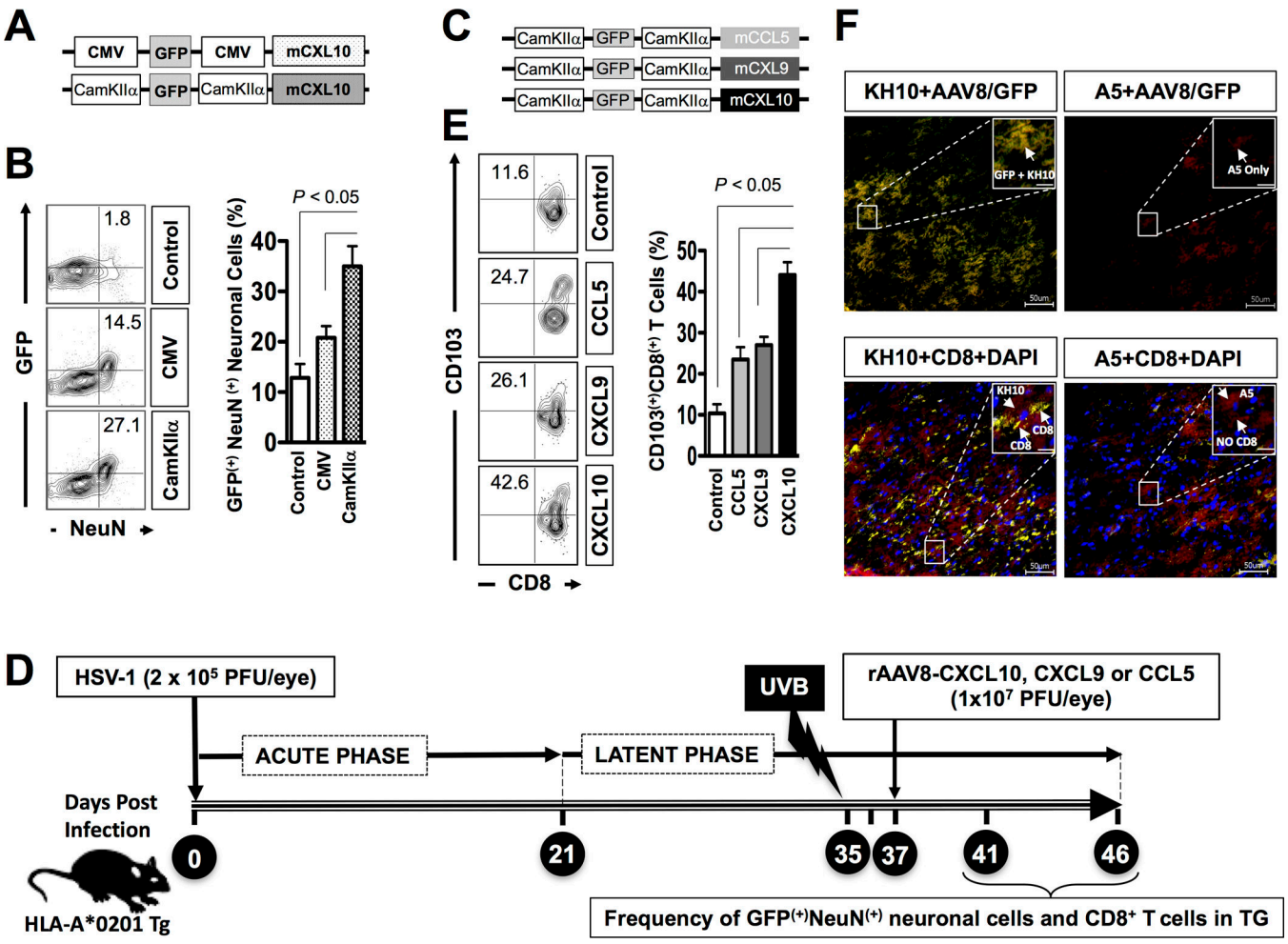

Figure 5. Delivery of chemokine-encoding recombinant non-replicating AAV8 vectors to latently infected trigeminal ganglia following ocular administration

(**A**) Schematic diagram of three AAV8 vector constructs expressing one of three different chemokines (i.e. CCL5, CXCL9 or CXCL10) and a GFP both under the neurotropic CamKIIα promoter. (**B**) Representative FACS plot of frequency of GFP positive neuronal cells ($GFP^{(+)}NeuN^{(+)}$ cells) in TG of mice (n = 10/group) that received topical ocular application of: (1) a rAAV-8-CMV-GFP-CMV-CXCL10 vector (*CMV*); (1) a rAAV-8-CamKIIα-GFP-CamKIIα-CXCL10 vector (*CamKIIα*); during HSV-1 latency (i.e. 41 dpi). Bar diagram show average frequency of $GFP^{(+)}NeuN^{(+)}$ cells in TG. (**C**) HLA-A*0201 Tg mice were ocularly infected with 2×10^5 pfu HSV-1 (strain McKrae). During latency (day 35 post infection), eyes of all mice were exposed to UV-B light. Forty-one dpi, mice (n = 10/group) received topical ocular application of: (1) AAV8-CamKIIα-mCCL5-CamKIIα-eGFP vector (*CCL5*); (2) AAV8-CamKIIα-mCXCL9-CamKIIα-eGFP (*CXCL9*); or of (3) CXCL10 (AAV8-CamKIIα-mCXCL10-CamKIIα-eGFP (*CXCL10*). Eye swabs were collected for 5 days following chemokine administration. On day 46-post infection, mice from all 4 groups were sacrificed and the frequencies of HSV-specific tissue resident memory $CD103^+CD8^+$ T_{RM} cells were evaluated in trigeminal ganglia. (**D**) Representative FACS plot of TG-resident $CD8^+$ T cells (*left*). Bar diagram of average frequency of TG-

resident $CD8^+$ T cells in TG of mice following delivery of three different chemokines (*right*). (**E**) Localization of GFP expression in two different types of sensory neurons (A5 and KH10) in TG of mice that received rAAV-8-CamKIIα-GFP-CamKIIα-CXCL10 vector. Mouse TG sections were co-stained using a mAb specific to KH10 (*left two panels*) or A5 (*right two panels*) sensory neurons, together with GFP (*upper two panels*) or with a mAb specific to mouse CD8 (*lower two panels*). Top two panels show immunofluorescence co-localization of $KH10^+$ neurons with AAV8-GFP detected using a Keyence BZ-X700 fluorescent microscope at 40× magnification and imaged using z-stack. The bottom two panels show immunofluorescence co-localization of KH10 and A5 with $CD8^+$ T cells. (Blue: DAPI, Red: neuron ($A5^+$ or $KH10^+$), Green: GFP-AAV8, Yellow: CD8). Bars in large box = 50 um. Bars in large box = 100 um. The results are representative of 3 independent experiments.

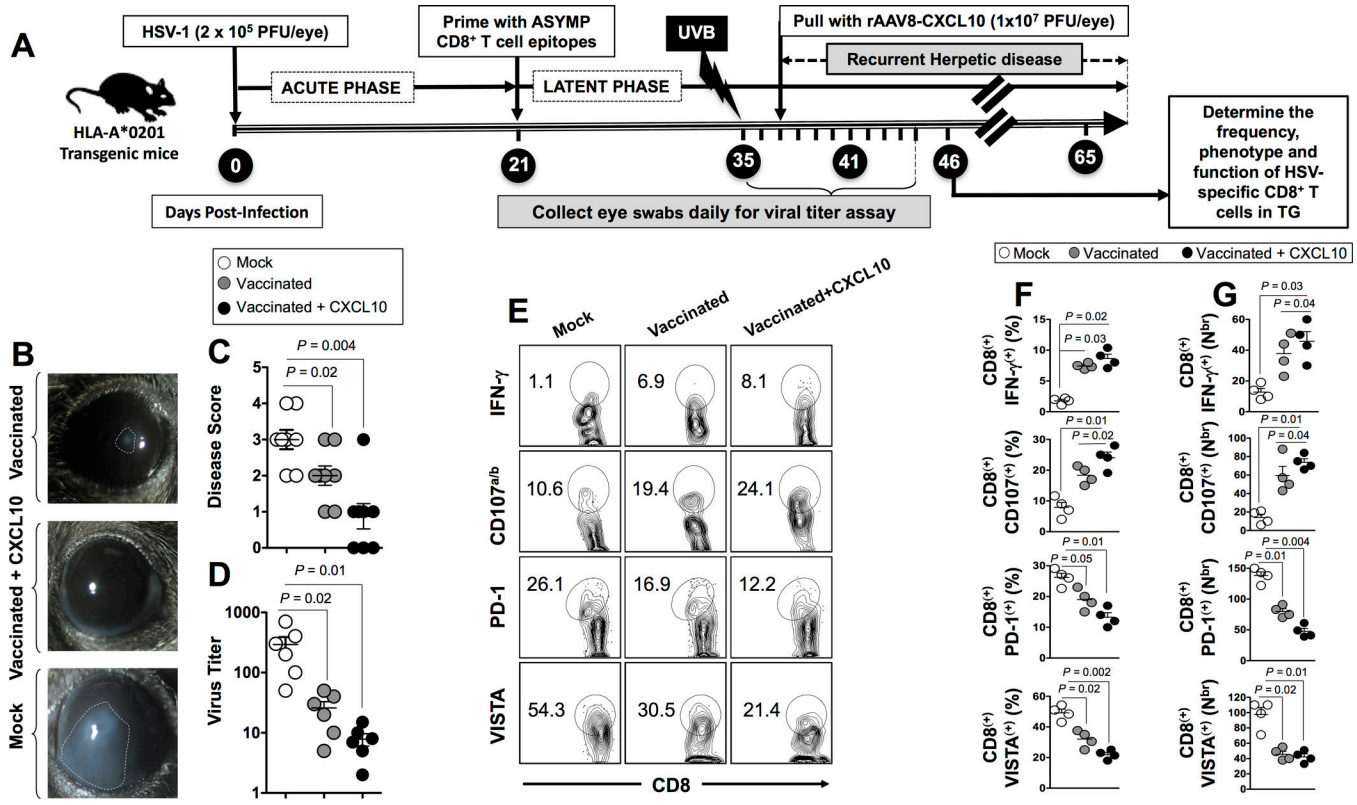

Figure 6. Protective immunity against recurrent ocular herpes induced by prime/pull therapeutic vaccine in latently infected HLA-A*0201 Tg mice

(**A**) Schedule of prime/pull therapeutic vaccination in HSV-1 infected HLA-A*0201 Tg mice. HLA-A*0201 Tg mice (6 – 8 weeks old, $n = 30$) were ocularly infected using 2×10^5 pfu HSV-1 (strain McKrae). 21-days post-infection, once the latency is well established, mice were divided in three groups ($n = 10$ each). Group 1 and group 2 were vaccinated with genome-wide derived ASYMP $CD8^+$ T cell epitopes ($UL9_{196–204}$, $UL25_{572–580}$ and $UL44_{400–408}$) along with PADRE $CD4^+$ T helper epitope both mixed with CpG_{1826} adjuvant. Group 3 mice received adjuvant alone (*Mock*). Two weeks after the first peptide vaccination (i.e. day 35 post infection), eyes of all three groups of mice were exposed UV-B light to induce reactivation. The eyes of all groups were swabbed daily up to 5-days post UV-B exposure with moist, type 1 calcium alginate swabs. Animals were examined for signs of ocular disease by slit lamp for 30 days. The recurrent herpetic disease was scored according to a standard 0 to 4 scale: 0, no disease; 1, 25%; 2, 50%; 3, 75%; and 4, 100% disease. On day 41 post infection, Group 1 of vaccinated mice ($n = 10$) was left untreated (*Vaccinated*) while Group 2 of vaccinated mice ($n = 10$) received topical ocular application of AAV8-CamKII-mCXCL10-CamKIIa-eGFP neurotropic vector (*vaccinated + CXCL10*). Eye swabs were collected for five additional days. (**B**) Top panel shows an eye picture of a mouse vaccinated with ASYMP epitopes + PADRE, without CXCL10 treatment (*Vaccinated*). Middle panel shows an eye picture of a mouse vaccinated with ASYMP epitopes + PADRE + treatment with CXCL10 chemokine (*Vaccinated + CXCL10*). Bottom panel shows the eye picture of a mock-vaccinated mouse control (*Mock*). (**C**) Average disease scores, on the scale of 0 to 4, detected in all three groups of mice. (**D**) Virus titer

detected in tears of all three groups of mice following UV-B induced reactivation. Five days after CXCL10 treatment (i.e. on day 46 post infection), mice from all groups were scarified and their TG extracted. The frequency, function and phenotype of HSV-specific $CD8^+$ T cells were evaluated in trigeminal ganglia of mice from all 3 groups. (**E**) Representative FACS plot of the frequency of "ASYMP" $UL9_{196–204}$ epitope-specific IFN-$\gamma^{(+)}CD8^+$ T cells; $CD107^{a/b(+)}CD8^+$ T cells; PD-$1^{(+)}CD8^+$ T cells and $VISTA^{(+)}CD8^+$ T cells detected in the TG of *Vaccinated*; *Vaccinated+CXCL10*; and *Mock-Vaccinated* mice. Average percentages (**F**) and average numbers (**G**) of "ASYMP" epitopes-specific IFN-$\gamma^{(+)}CD8^+$ T cells; $CD107^{a/b(+)}CD8^+$ T cells; PD-$1^{(+)}CD8^+$ T cells and $VISTA^{(+)}CD8^+$ T cells detected in the TG of *Vaccinated*; *Vaccinated+CXCL10*; and *Mock-Vaccinated* mice. The nominal *P* values indicated on panels (**C**), (**D**), (**F**) and (**G**) show statistical significance between vaccinated and mock-immunized mice. We have used the General Linear Model procedure and compared the least squares means using the Dunnett procedure for multiple comparisons.

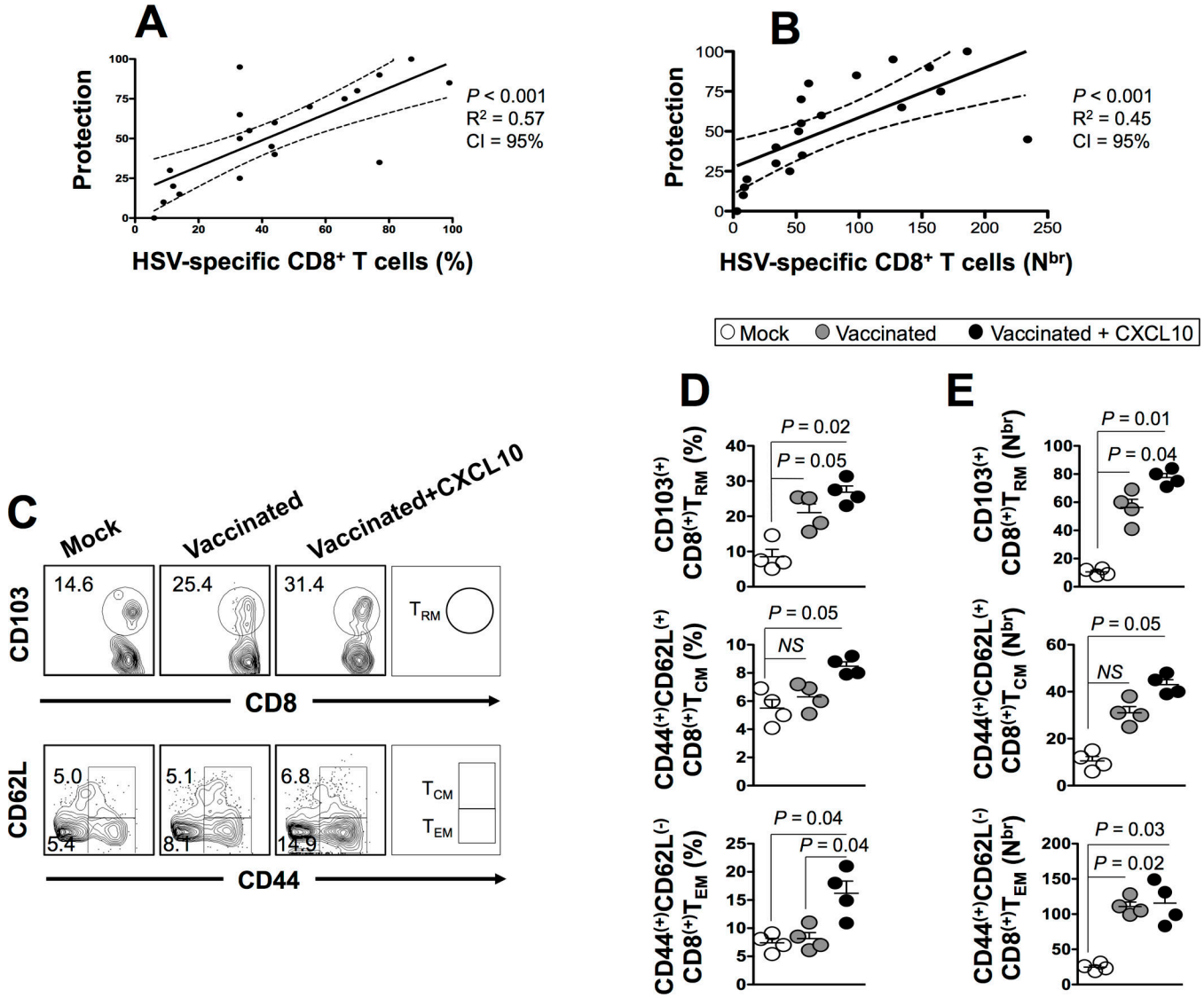

Figure 7. Bolstering the number of HSV-specific CD8$^+$ T_{CM}, T_{EM} and T_{RM} cells in trigeminal ganglia of latently infected HLA-A*0201 Tg mice following the prime/pull therapeutic vaccine reduces recurrent herpes infection and disease

The trigeminal ganglia were harvested from all groups of mice (vaccinated and non-vaccinated) and single cell suspension from TG were obtained after collagenase treatment for an hour at 37°C and stained for markers of total CD8$^+$ T cells, CD8$^+$ T_{RM}, T_{CM} and T_{EM} cell sub-populations. Positive correlation of the percentage (**A**) and number (**B**) of HSV-specific CD8$^+$ T cells in TG with protection against ocular herpes. (**C**) Representative FACS plot of the frequency of "ASYMP" $UL9_{196–204}$ epitope-specific CD103$^+$CD8$^+$ T_{RM} cells (*top panels*); $CD44_{high}CD62L^{high}CD8^+$ T_{CM} cells (*middle panels*); and $CD44_{high}CD62L^{low}CD8^+$ T_{EM} cells (*bottom panels*) detected in the TG of *Vaccinated*; *Vaccinated+CXCL10*; and *Mock-Vaccinated* mice. Average percentages (**D**) and average numbers (**E**) of "ASYMP" epitopes-specific CD103$^+$CD8$^+$ T_{RM} cells (*top panels*); $CD44_{high}CD62L^{high}CD8^+$ T_{CM} cells (*middle panels*); and $CD44_{high}CD62L^{low}CD8^+$ T_{EM} cells (*bottom panels*) detected in the TG of *Vaccinated*; *Vaccinated+CXCL10*; and *Mock-*

Vaccinated mice. The results are representative of 2 independent experiments. The nominal *P* values indicated on panels (**D**) and (**E**) show statistical significance between vaccinated and mock-immunized mice. We have used the General Linear Model procedure and compared the least squares means using the Dunnett procedure for multiple comparisons.

Table 1

Cohorts of HLA-A*02:01 positive, HSV seropositive Symptomatic and Asymptomatic individuals enrolled in the study

(**A**) Total HLA-A*02:01 positive, HSV seropositive Symptomatic and Asymptomatic individuals screened. (**B**) HLA-A*02:01 positive, HSV seropositive Symptomatic and Asymptomatic individuals enrolled in this study. Definition of Symptomatic and Asymptomatic individual is detailed in *Materials and Methods*.

A

Subject-level Characteristic	All Subjects (n= 803)
Gender [no. (%)]:	
Female	410 (51%)
Male	393 (49%)
Race [no. (%)]:	
White	554 (69%)
Nonwhite	249 (31%)
Age [median (range) yr.]:	39 (21–67 yr.)
HSV status [no. (%)]:	
HSV-1-positive	293 (36%)
HSV-2-positive	376 (47%)
HSV-1- & 2-positive	36 (4%)
HSV-negative	98 (12%)
HLA [no. (%)]	
HLA-A*02:01-positive	422 (53%)
HLA-A*02:01-negative	381 (47%)
Herpes Disease Status [no. (%)]	
ASYMPTOMATIC (ASYMP)	658 (91%)
SYMPTOMATIC (SYMP)	64 (9%)

B

Subject-level Characteristic	Enrolled Subjects (n= 38)
Gender [no. (%)]:	
Female	20 (52%)
Male	18 (48%)
Race [no. (%)]:	
White	24 (63%)
Nonwhite	14 (37%)
Age [median (range) yr.]:	39 (21–67 yr.)
HSV status [no. (%)]:	
HSV-1-positive	28 (73%)
HSV-2-positive	0 (0%)
HSV-1- & 2-positive	0 (0%)
HSV-negative	10 (27%)

B

Subject-level Characteristic	Enrolled Subjects (n= 38)
HLA [no. (%)]	
HLA-A*02:01-positive	28 (73%)
HLA-A*02:01-negative	10 (27%)
Herpes Disease Status [no. (%)]	
ASYMPTOMATIC (ASYMP)	18 (64%)
SYMPTOMATIC (SYMP)	10 (36%)